Electrostatic Separators

for Muon Colliders

Rolland Johnson,
Muons, Inc.

Why consider Electrostatic Separators?

- If more than 1 on 1 bunches are needed. e.g.
  - Large single bunch intensities are impossible
    - RF beam loading
    - Space charge limitations
    - Instabilities
  - Too many interactions/collision
    - Detector trigger or background limitations
  - Topping-up can increase average luminosity

- Then electrostatic beam separators can be used
  - Alternative to having a ring for each muon charge sign
  - Used at the Tevatron
    - (déjà vu! Talk from 5/4/1986, exactly 21.5 years ago!)

A SCHEME FOR 5×10^{31} IN THE TEVATRON

Features:

many bunches to minimize
    # interactions/crossing

TeV I source design parameters
    $10^{11} \bar{p}/h$, $10^{12} \bar{p}$ max in Accum.

Uses Tevatron as additional accumulator

A SCHEME FOR $\mathcal{L} = 5 \times 10^{31} \, cm^{-2} s^{-1}$
IN THE TEVATRON

Features:

~ Many bunches to minimize the number of interactions / crossing

– electrostatic separators in both planes to reduce number of crossings (to control beam-beam tune shift)

– shuttered injection / abort kickers to allow proton beam replacement. e-s separators used here, too.

– new low β insertion with e-s separators ($\frac{1}{4}$ m)

– acceleration / deceleration operation to allow proton replacement and $\bar{p}$ addition or refreshment. Can use the Tevatron as an additional accumulator.

Numbers of bunches:

$$\frac{N_{ints}}{Xing} = \frac{\Sigma\sigma}{n_b f_{rev}}$$

for $\overset{144}{1\cancel{5}0} \times \overset{144}{1\cancel{5}0}$, $\frac{N_{ints}}{Xing} \sim \frac{2}{3} = .73$

100 mB, 5×10^{31}

$$\frac{}{\text{why } 1\cancel{\overset{144}{5}}0 ?}$$ Jim Griffin will tell.

$$1113 = 3 \times 7 \times 53$$

every 7th rf bucket gives
159 bunches, leave $\overset{15}{\cancel{X}}$ out for end
effects.   ($132\,$ns twixt $\overset{most}{crossings}$)

---

1 bunch/12 rf buckets is also a
possibility, but since we have a
scheme for the 1/7 case and more
bunches is better.....

Electrostatic Separators

needed to reduce the number of head-on
bunch crossings (here $3/IR \Rightarrow 6$)
with $B\phi$ and $D\phi$ only
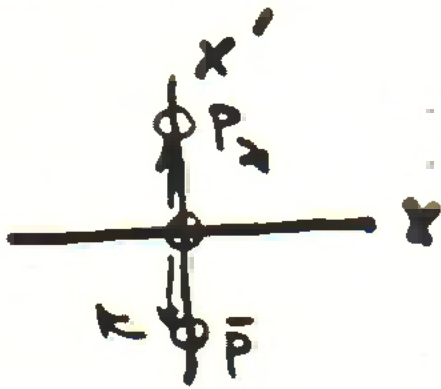
$$x' \approx \Theta = \frac{eVl}{E}$$

practical experience $\Rightarrow$ $V \lesssim 50 KV/cm$

injection
$\rightarrow$ so $5m$ of $50 KV/cm \Rightarrow \sim 770 \mu r$ Kick
at $150 GeV$

low β
$\rightarrow$ or $4m$ at $1 TeV$

$\Rightarrow 20 \mu r$

$$\xi(z) = \Theta \frac{\sqrt{\beta_s \beta(z)}}{2 \sin \pi \nu} \cos\left(\left|\Psi_{SIP} - \Psi(z)\right| - \pi\nu\right)$$

$$\ell \sim 1.9$$

$$= \pm 2.3 \, mm \quad \text{for } 20\mu r \text{ if } \beta_s = 500 \, m$$
$$\text{if } \beta(z) = 100 \, m$$

$$\sigma(z) = \sqrt{\epsilon \beta(z)} = 0.56 \, mm \quad, \quad \epsilon = 20\pi$$
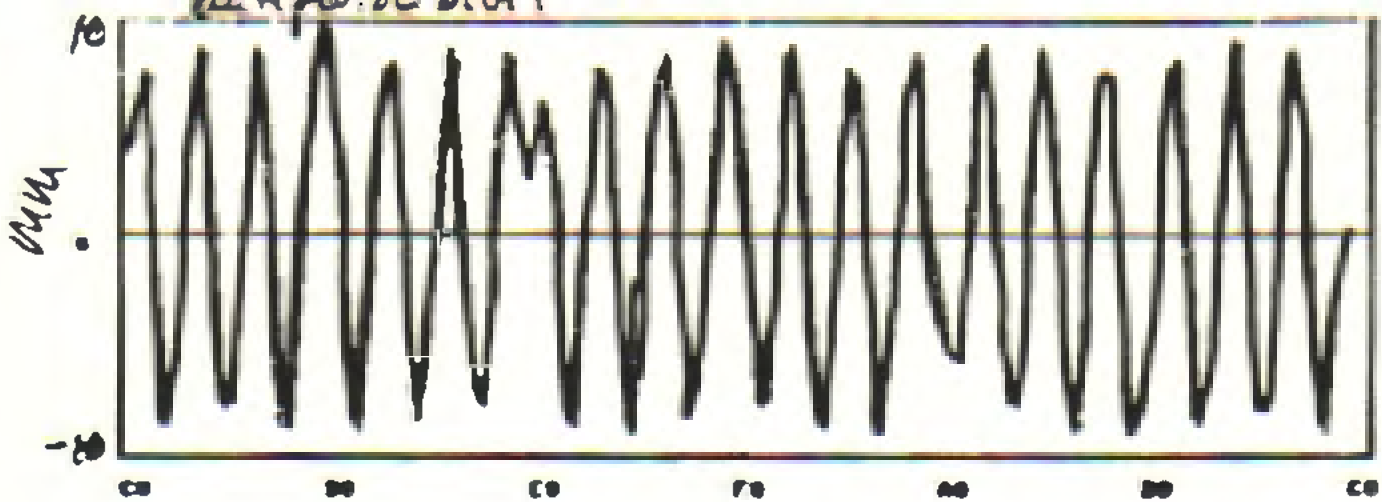$$\beta(z) = 100 \, m$$

$$n_\sigma = \frac{\xi}{\sigma} = \frac{\Theta}{2 \sin \pi \nu} \sqrt{\frac{\beta_s}{\epsilon}} \cos\left(\left|\Psi_s - \Psi\right| - \pi\nu\right)$$

$$= \pm 4.1 \qquad \left(\begin{array}{c}\text{CERN GETS BY} \\ \text{WITH } \pm 2.6 \text{ IN ONLY} \\ \text{ONE PLANE}\end{array}\right)$$

COMMENTS:
- NEW IDEA. USE THE HIGH β CLOSEST TO THE IR
TO GET EFFECTIVE SEPARATORS WHILE GETTING THE
BEAMS SEPARATED AS SOON AS POSSIBLE TO MINIMIZE
HEAD-ON CROSSINGS. (3 / IR + (B∅ + D∅) = 6 total
- GO TO LOW β WITH INJECTION OPTICS (NO HEAD-ON)
... QUICKLY TO COLLISION SEPARATION SCHEME (< 10°.

H Calculated Positions (mm)

ES KICK
200 μr

shuttered
Kicker location

There will be 2 separators, one in each
plane with 90° phase advance between.

After the beams have been injected,
the shutter is removed, the beams are accelerated
to 1 TeV. The "cusps" in the 2 planes stay on
until the low β is on. There are no head-on
collisions until the separators at the IRs
are turned on.

H Calculated Positions (mm)

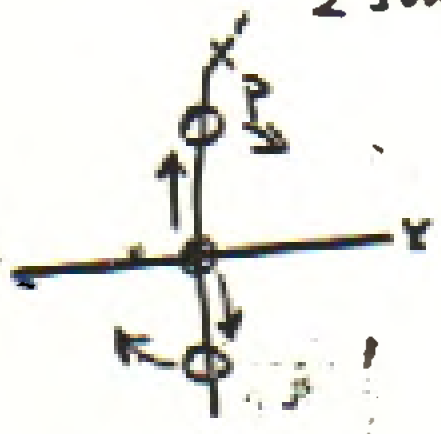|	C	D	E	F	A	B
11	-4.137	-8.244	-4.314	-2.544	5.430	4.843
13	-7.795	3.595	-4.529	7.413	9.703	-4.947
15	1.051	0.092	8.476	7.448	-4.307	-0.941
17	8.596	3.006	(1.651)	-1.707	-0.906	-.1257
19	5.400	-0.375	1.833	-0.022	-8.374	8.304
22	-4.532	-0.039	-7.800	-4.829	7.130	6.303
24	-0.805	.5626	-4.954	5.142	7.767	-3.692
26	-2.072	0.432	2.650	0.720	-1.264	-9.800
29	7.250	5.702	0.957	1.374	-0.733	-2.002
32	7.307	-4.092	4.077	-7.711	-3.423	6.919
34	-1.642	-0.062	-5.910	-7.178	4.792	7.909
36	-0.719	-2.358	-8.300	2.336	8.034	-.9434
38	-4.962	6.936	-.4468	0.072	1.875	-8.679
42	4.999	7.779	8.140	4.307	-7.455	-8.613
44	0.704	-1.036	6.570	-5.430	-7.465	4.489
46	1.359	-0.595	-3.109	-0.890	1.640	8.750
48	-7.603	-5.532	-9.102	-.9441	9.074	2.301
49	-12.61	-2.675	-7.634	2.190	7.931	-.3072

TEVATRON

AVERAGE =	-.213092
RMS =	6.30171
RMS/(MEAN) =	6.30409
MAXIMUM =	12.6131
AT	C49
MAX/RMS = (MEAN)	2.02406

200 μr
at
D49

$$X(z) = \frac{\Theta \left(\beta_{sep} \beta(z) \right)^{1/2}}{2 \sin \pi \nu} \cos \left(\left| \psi_{sep} - \psi(z) \right| - \pi \nu \right)$$

$$x' \sim \Theta = \frac{e V \ell}{E} \qquad V \lesssim 50 \, KV/_{cm}$$

Injection 6 m @ 50 KV/cm
———————————————————
150 GeV ⟹ 200 μr of kick

Low β 4m @ 50 KV/cm,
1 TeV ⟹ 20 μr kick

TOM. Ferdi Willeke soln

(1 more than at 3.4 now)
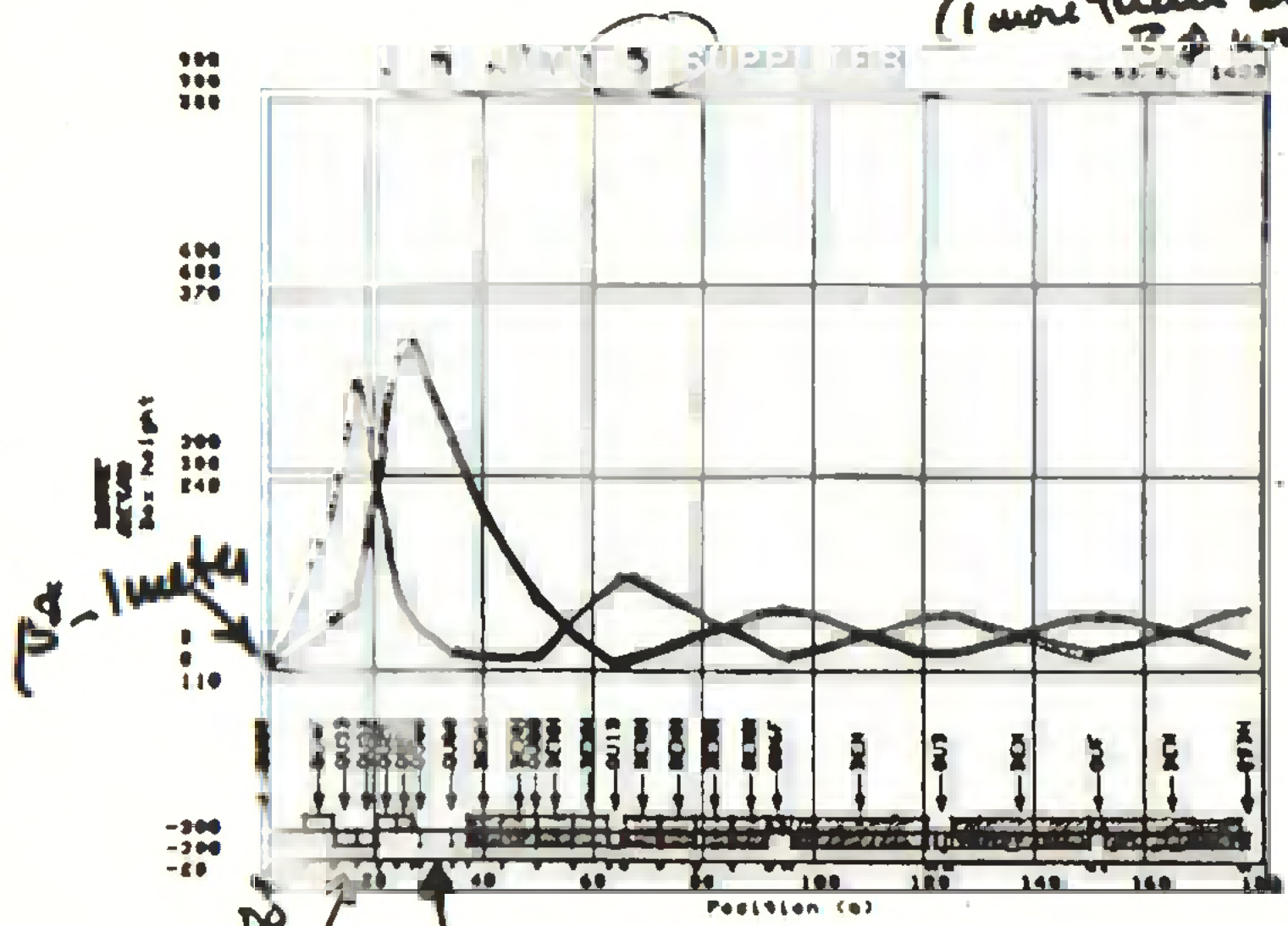
"Collins quads" removed for es separators

Dave Finly

The Double Helix

at 1st separation

at next separation
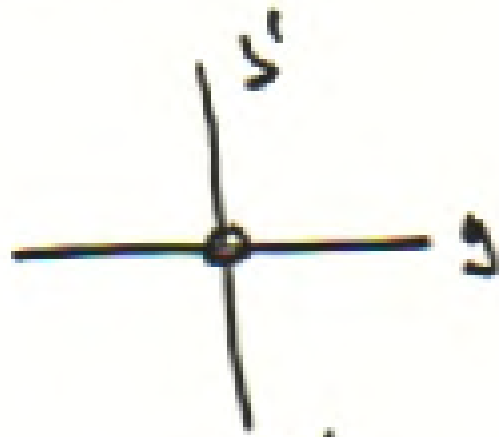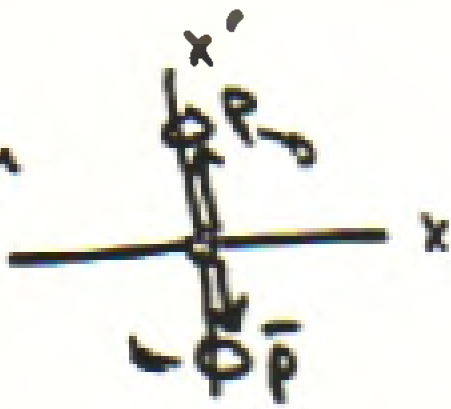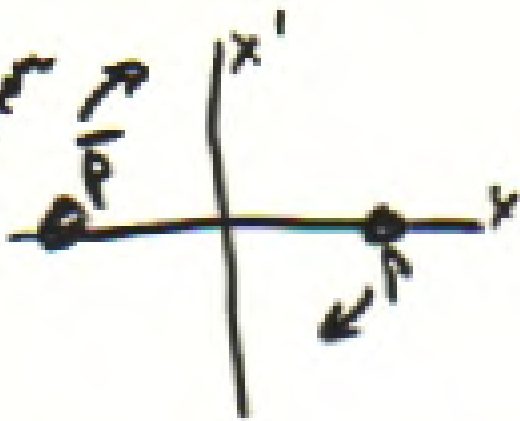
and so on through the arcs to the next low p

at final r sep
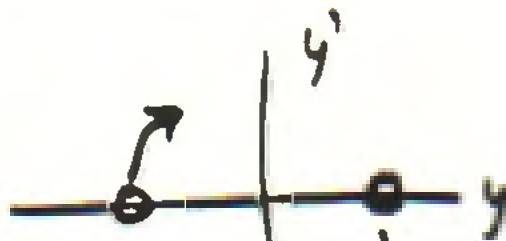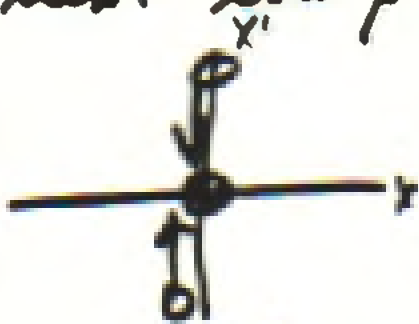
at final y separation
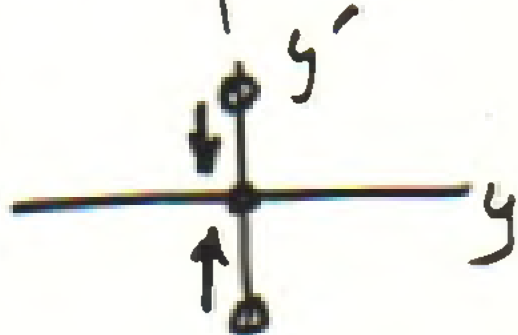
In general, there are not multiples of π phase advance and another pair of separators are needed to make honest 3-bumps in each plane.

1 M WITH 5 SUPPLIES
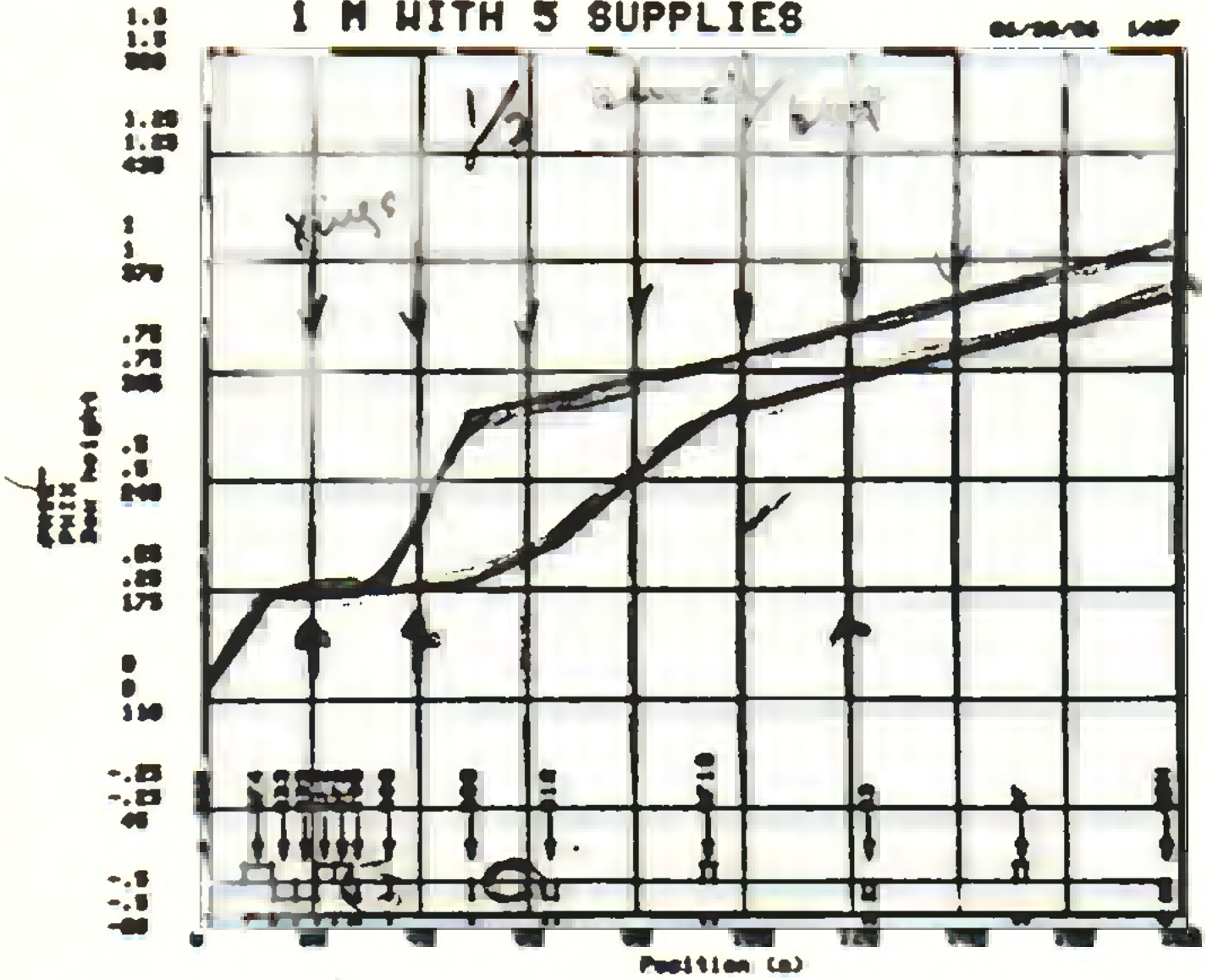
Strategy 1 : longitag at collins quad locu.

B0/D0 LOW BETA PROPOSAL

IDENTITY OF B0 AND D0

"INDEPENDENCE" OF B0 AND D0

(ARC MATCHING QUADS)

$$225 \ CM > \beta^* > 18 \ CM$$

$$- 4 \ DEGREES \ GETS \ TO \ \beta^* = 44 \ CM$$

$$- 1.8 \ DEGREES \ GETS \ TO \ 18 \ CM$$

D0 COLLIDER VS FIXED TARGET

MR   P→   LAM

(LAB KICKER)
                    D49

TEV   LAM

                                              E11

                                                         E17
                                                      KICKER
                                                      SHUTTERED

Fe   45°   EØ

                              bumped
                              orbit

                                    P   E11 LAMBERTSON

                              normal
                              circulating
                              beam
injected
beam   P

coasting
P beam   3mm

        P   shutter

                                                    E17
8.5mm   8.5   x

                                              injection
                                              kicker
                              injected   P   35°

12π 95% E
    shown
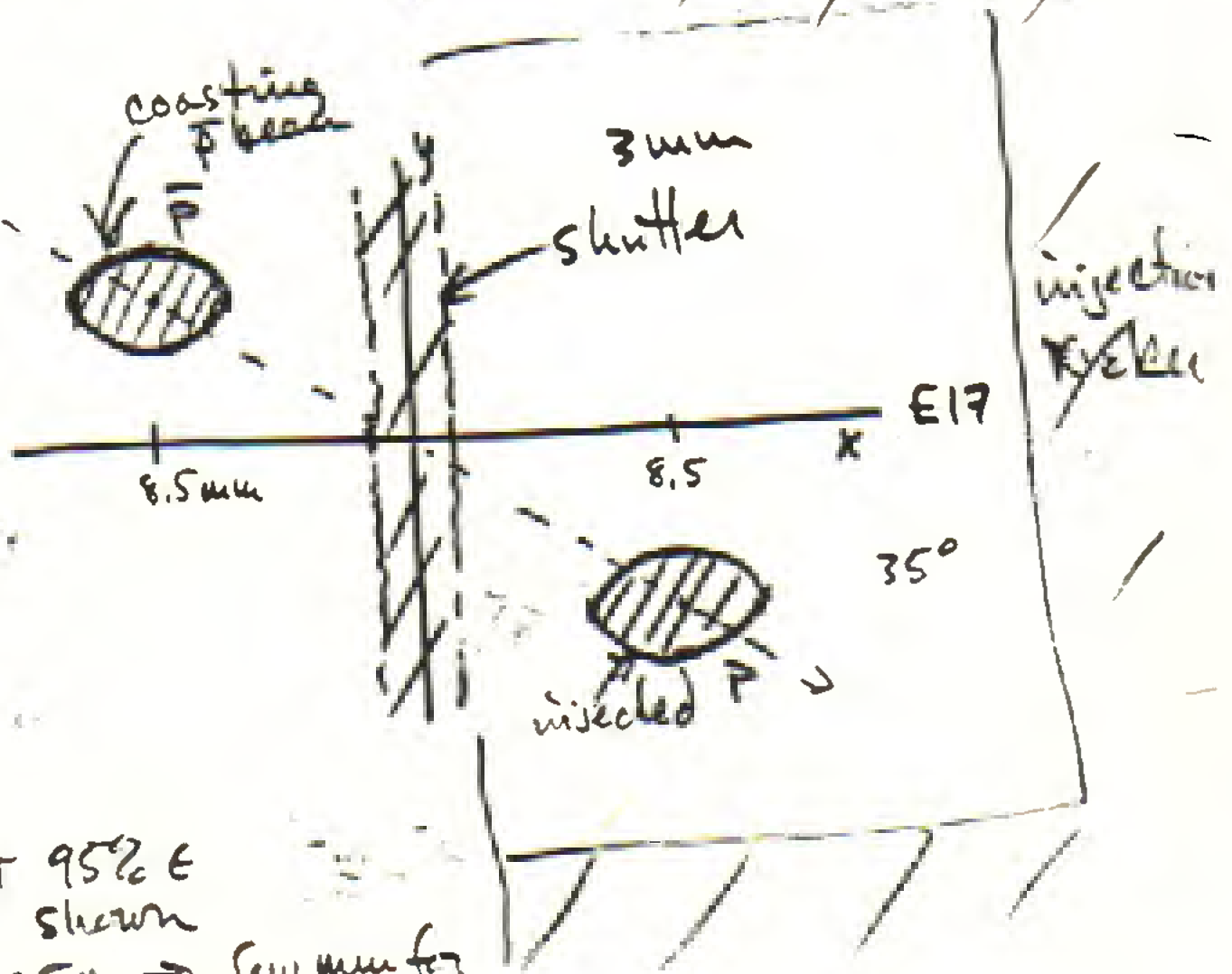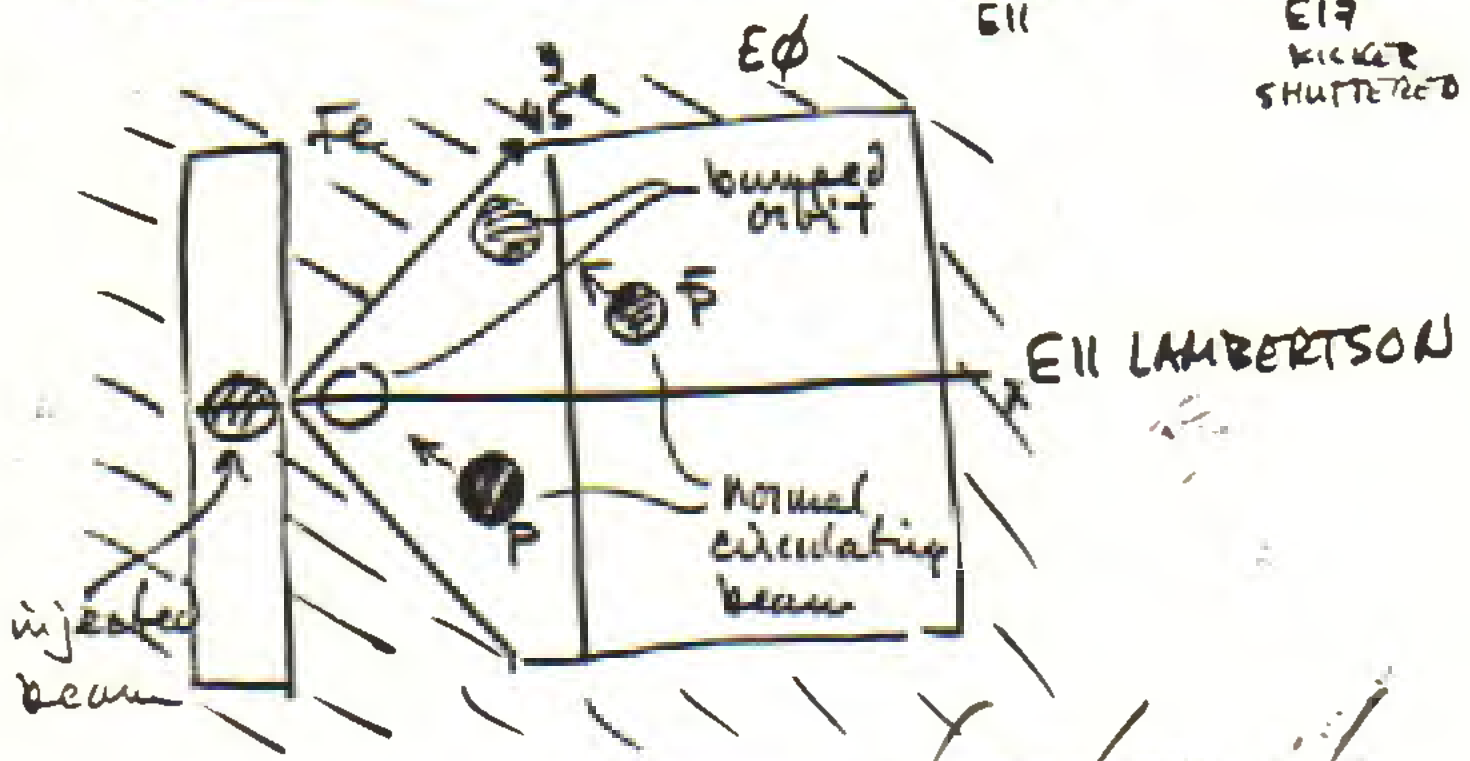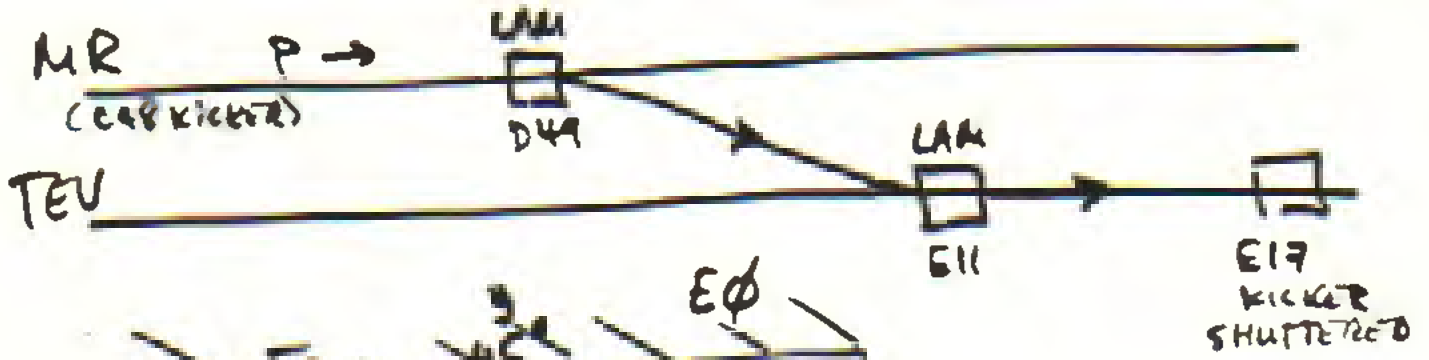
Transverse Lattice Functions

(44 cm beta* at B0 and D0, tunes 20.42,20.41)

Legend: — Hor Beta, — Ver Beta

Y-axis: meters (1000, 800, 600, 400, 200, 0)

X-axis: Path Length (meters) (0, 1000, 2000, 3000, 4000, 5000, 6000)

Ao
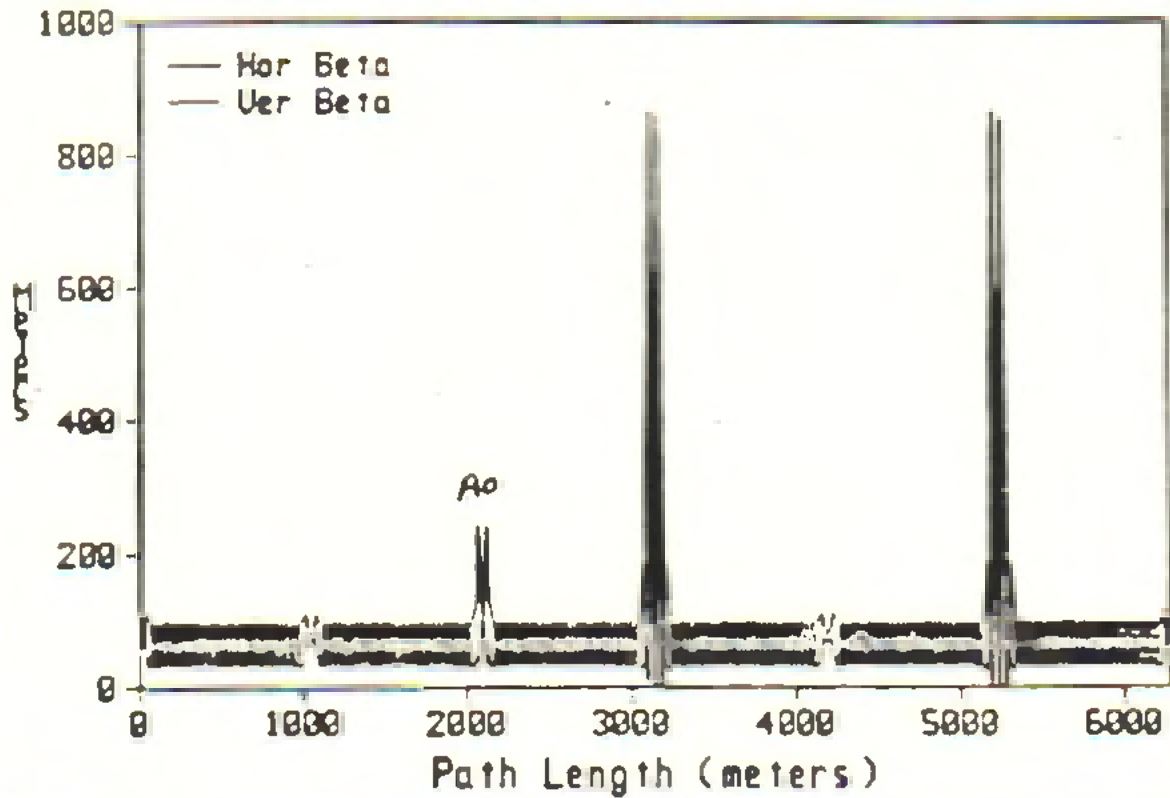
Transverse Lattice Functions

(1986 lattice without arc matching quads)

Legend: — Hor Beta, — Ver Beta

Y-axis: meters (1000, 800, 600, 400, 200, 0)

X-axis: Path Length (meters) (0, 1000, 2000, 3000, 4000, 5000, 6000)

Ao

Beam-Beam

E_y vs x/σ
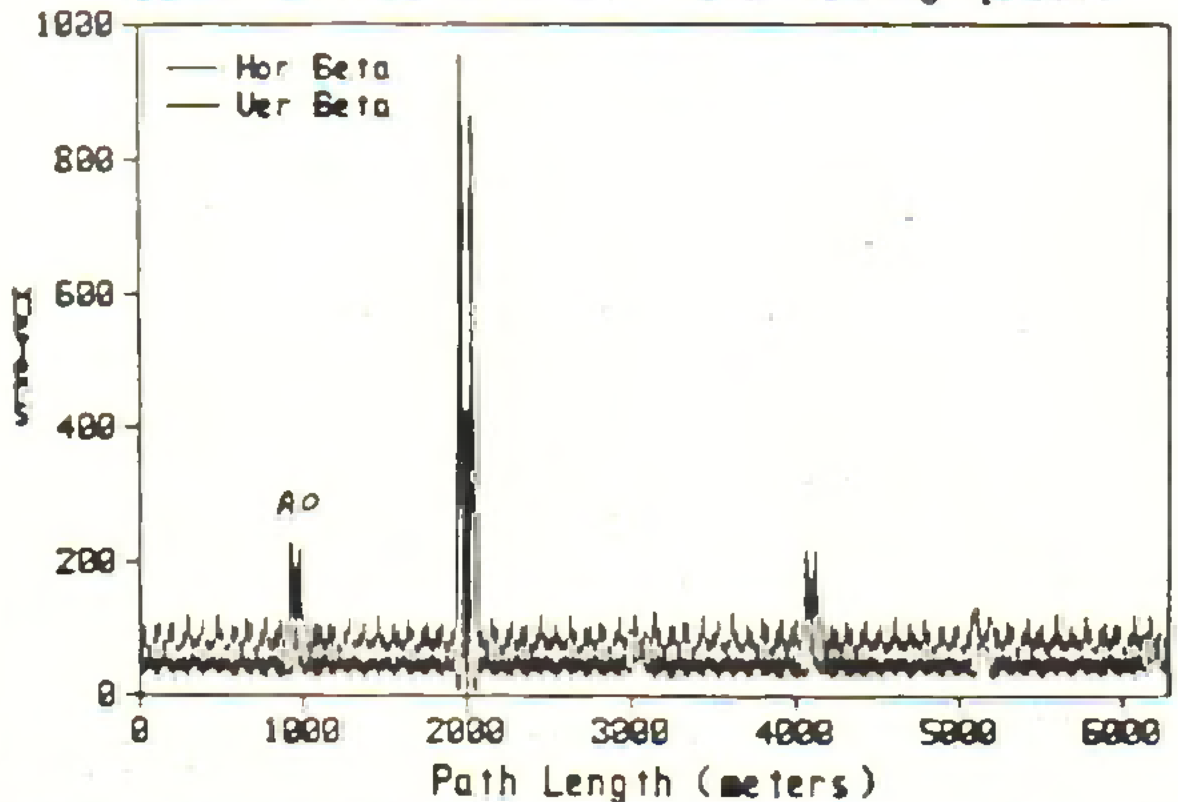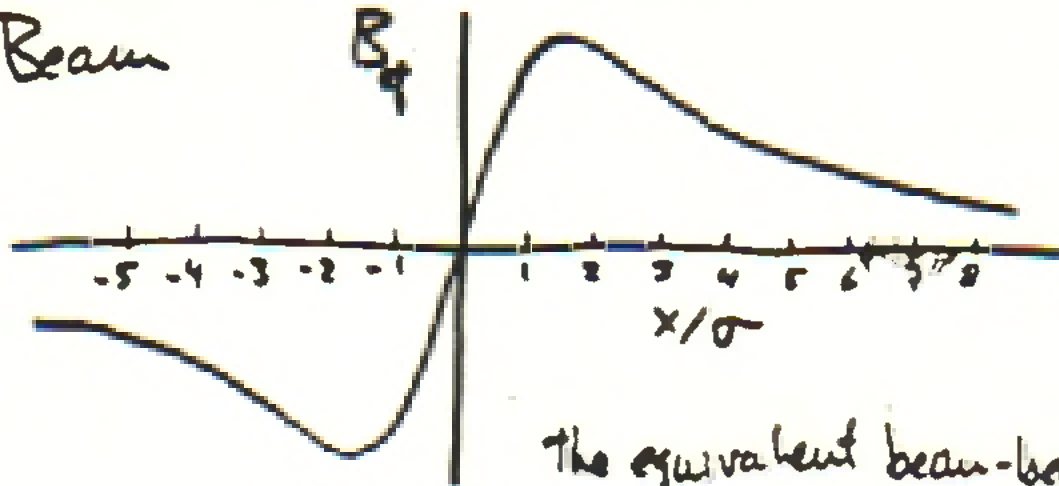
the equivalent beam-beam field

for $\frac{v}{c} \sim 1$, $eE \sim evB$

For small x, (head on) only 6 crossings.

Multipole Expansion — Long-range effects (passings)

for $r \gg$ beam radius

$$E = \frac{2e\lambda}{r}$$

λ linear density

let $r \to r_0 + x$

$$E = \frac{2e\lambda}{r_0 + x} = \frac{2e\lambda}{r_0}\left(1 - \frac{x}{r_0} + \frac{x^2}{r_0^2} - \frac{x^3}{r_0^3} + \cdots\right)$$

need to consider each term's effect at each energy.

Beam-Beam, long range cont.

1. Dipole Effect

$$\text{Force} \hat{=} 2eE = \frac{4e^2\lambda}{r_0} = m\gamma\frac{d^2x}{dt^2} = mc^2\gamma\frac{d^2x}{ds^2}$$

$$\delta x' = 4\frac{e^2}{mc^2}\frac{1}{\gamma r_0}\int \lambda\, ds = 4r_p\frac{N}{\gamma r_0}$$

$$N = 6\times10^{10}$$
$$r_0 = 5\,mm = .005\,m$$
$$\gamma = 1067 \quad @1\,TeV$$
$$r_p = 1.535\times10^{-18}\,m$$

$$\delta x' = 6.9\times10^{-8} \underset{1TeV}{} = \underset{150GeV}{} 46\overset{13}{}\times10^{-8}$$

but $2\times144 - 6 = 282$ nearby collisions,
half x, half y acting incoherently $\Rightarrow$

$$\Delta x' = \sqrt{\frac{282}{2}}\,\delta x' = 8.2\times10^{-7}\underset{1TeV}{} = .8\mu r$$

$$= 1.5\mu r \;_{150\,GeV}$$

Compare to 20μr delta seps at 1 TeV
" " 200 μr " " " " " 150 GeV

$\sim 5\%$ offcenter Double Halo ...

Beam-beam, long range etc.

2. Quadrupole effect

$$\delta x' = 6.9 \times 10^{-8} \frac{x}{r_0} \qquad \text{(per crossing)} \atop \text{passing}$$

$$\delta \nu = \frac{\beta x}{4\pi} \frac{\delta x'}{x} \qquad \beta_x \cong 50m$$

$$\Delta \nu_x = \cancel{\frac{1}{2}} .144 \; \frac{6.9 \times 10^{-8}}{.005} \; \frac{50}{4\pi} = \underline{.008}_{\quad 1\,TeV}$$

each plane

at 150 ⇒ .005

However, this is a tune shift (can be compensated)
        there is cancellation due to the
vertical and horizontal passages

Beam-beam, long range contd.

3. Sextupole and higher moments

Can compare kicks due to beam passages with those due to errors in superconducting dipoles.

in general, $\dfrac{288 \text{ Kicks from beam-beam}}{774 \text{ Kicks from dipole multipoles}}$

is $\lesssim 2\%$

$\Rightarrow$ Negligible or correctable

$\gamma = T_{eV}I$

$6E10$ p/bunch   144 bunches

$86E12$

N_p $\langle \frac{1}{\epsilon_H} \rangle$

$\tau_h \sim 12h$ INTRABEAM SCATTERING LIFETIME

$\gamma = T_{eV}s$

$3E10$ $\bar{p}$/bunch   144 bunches

$4.3E12$

$N_{\bar{p}}$ $\langle \frac{1}{\epsilon_H} \rangle$

$\tau_h = 24 hrs$

2 4 6 8 10 12 14 16 18 20 22 24

time (hours)
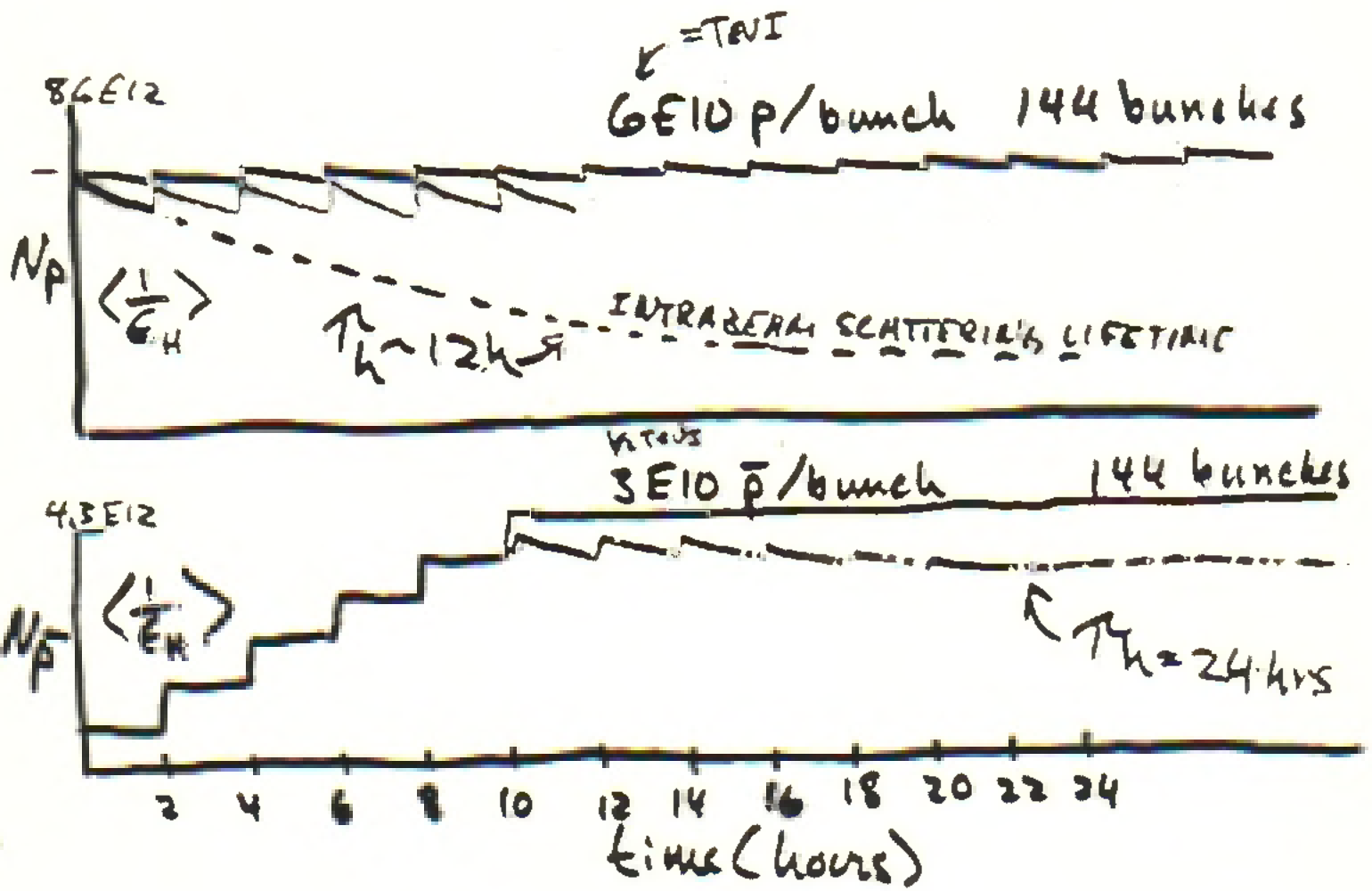
$\mathscr{L}_{peak} = 5.8 E31$ for asymptotic 20π $\perp$

$\beta^* = \frac{1}{2} m$

$\langle \mathscr{L} \rangle \gtrsim 5E31$

Figure shows luminosity $\mathcal{L}$ (cm^{-2} s^{-1} / 10^{30}) vs Bunch Length σ.

Plot parameters:
1 TeV
6E10 p's, 3E10 $\bar{p}$'s
144 on 144
20π mm-mrad
D*, D'* = 0
a* = 0

Curves labeled β*: 1/4 m, 1/2 m, 1m

Arrows labeled: 17 cm, 40 cm, 1985
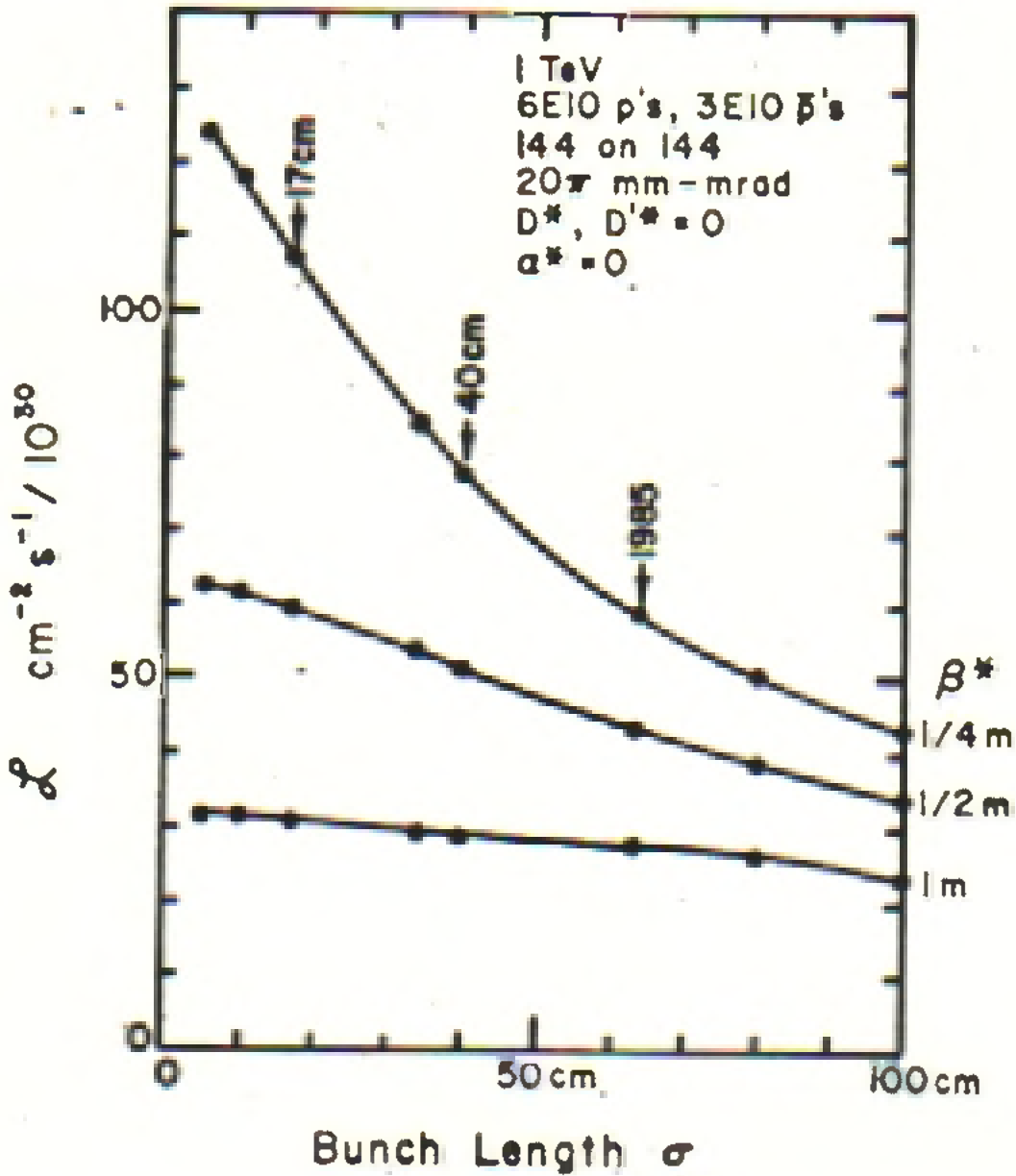
Effectiveness of low β depends on bunch length. One problem: shorter bunch length may lead to intrabeam scattering complications.

BUT! we can have a source at $4 \times 10^{11}\, \bar{p}/hr$ and 12π. Don't need such a stable Tevatron, can use less intense p bunches. Also less worries about intrabeam scattering.

$6\,E10\; p/bunch \qquad \overset{144}{\cancel{180}}\; bunches$

N_p

$T_{\frac{1}{2}} \sim 12h$

$3\,E10\; \bar{p}/bunch \qquad \cancel{180}\; bunches$

$N_{\bar{p}}$

$4.5\,E12\; \bar{p}$

$T_{\frac{1}{2}} = \frac{3 \times \, hrs}{24}$

time (hours)

2 4 6 8 10 12 14 16 18 20 22 24

$$\mathcal{L}_{peak} = 5.8 \times 10^{31} \text{ for asymptotic } 20\pi\,\epsilon$$

$$\beta^* = \tfrac{1}{2}\, m$$

$$\langle \mathcal{L} \rangle \approx 5 \times 10^{31}$$

HOW IT WOULD WORK FOR A TEV I $\bar{P}$ SOURCE

ie. $10^{11} \bar{P}/hr$, 10^{12} mag in core.

15π

2πRMS

1.2 E11 p/bunch   111 bunches

N_p

$\langle \frac{1}{\epsilon_H} \rangle$ $\tau_h = 12$ hrs

$\frac{1}{2}$ TeV I

0.3 E11 $\bar{p}$/bunch 111 bunches

$N_{\bar{p}}$

$\langle \frac{1}{\epsilon_H} \rangle$ $\tau_h = 48$

0   6   12   18   24   48   72

time hours

$\mathcal{L}_{peak} \sim 3E31$ Assuming a TeV I params

$\mathcal{L}_{min} \simeq \frac{2}{3}$ "   ie. $\beta^* = 1m$

$\mathcal{L}_{ave} \sim 2.5 E31$ $\epsilon_{95 \, ASYM} = 24\pi$

IF $\beta^* = \frac{1}{2}m$, $\langle \mathcal{L} \rangle = 5E31$

@ 3E31 $\tau_{coll \, \bar{p}} \sim 60$ hrs

This requires a very reliable Tevatron
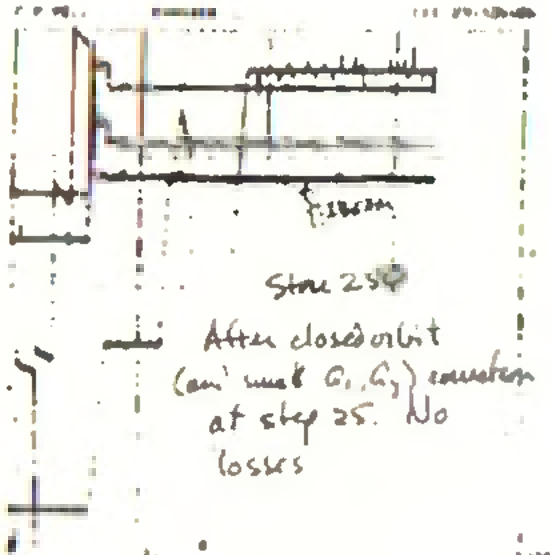
Store 25?

After closed orbit
(can't meet C_1, C_2) correction
at step 25. No
losses

0315 Go on to store 251 while TeV rf #3 be... looked at.
      see injection times of 0.446 and ...94 ← inject
      (Δ≈.012)   late

0318 GO TO LOW β
      GO TO FT LATTICE
0333 GO TO LOW β   } testing new f... ...ces of Till...
      GO TO FT LATTICE   (no beam ... ss — see FW
0347 GO TO LOW β   for proof ... ...ance decimte...
      GO TO FT LATTICE   }   — ...   ye...
0425 GO TO LOW β

0430 Okay — so we see no beam losses with cables ... ...ni. Even wh...
      we squeeze and unsqueeze the same beam 4 t... . flying wires
      show about 2% ... in the vertical, with no ... change of ...
      for VC45. The story for HC48 is more con... !

(note that TeV RF #3 is in need of repair - ... ...ided to wa...
      for daylight to call someone in)

0520 Store 25? ends. E1 BLM. Due to F17 HR ... ...tion lampets
      trip.

251

intensity

Q1
QU4...
currn...

same ...
low β o...

time ⇒
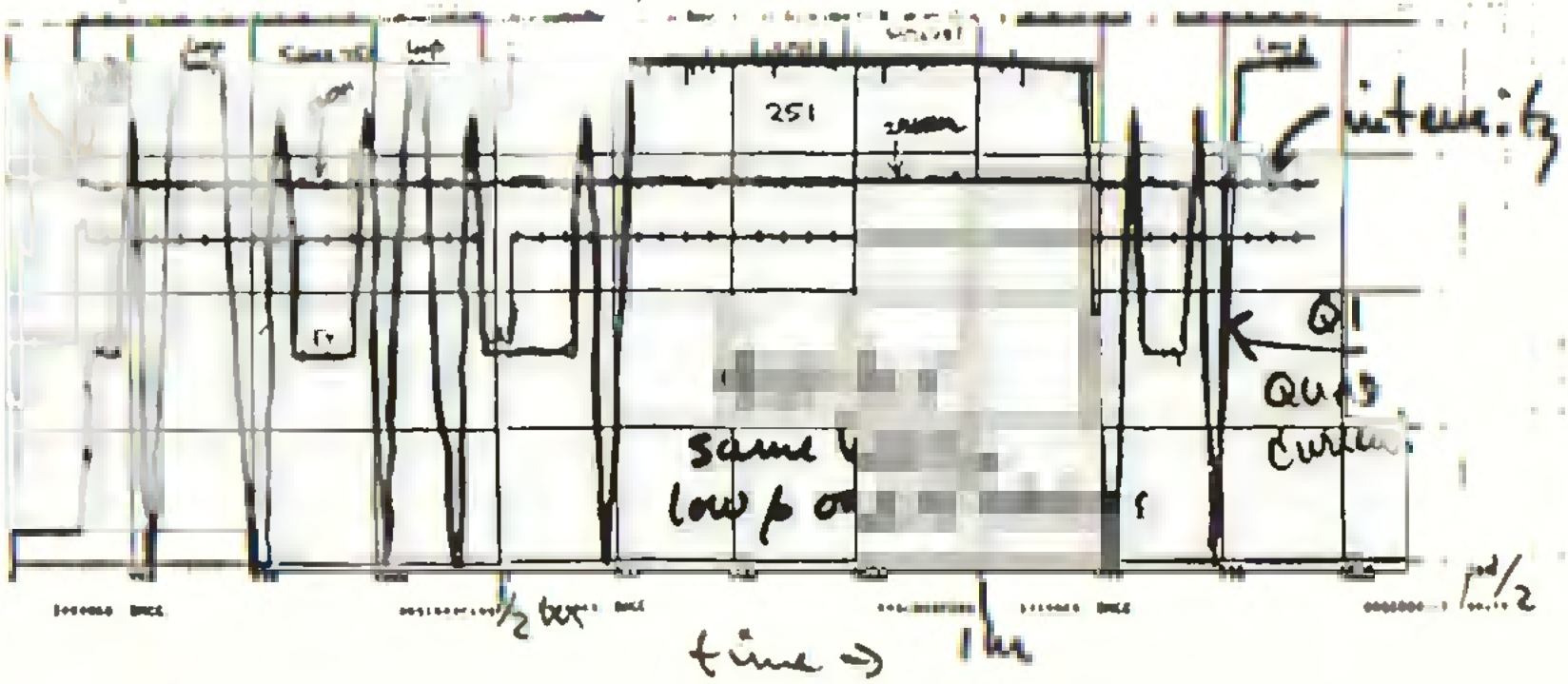
What has to be done for deceleration/ug

4 mins {
- turn off low β, Keep beams separated (switch to 2 aperture)
- decelerate, don't let losses quench magnets

1 min {
- Kill proton beam with shuttered abort
- add p̄ bars ≥ 2 MR cycles
- add protons $< \frac{MR}{2} = 1\frac{1}{2}$ MR cycles

5 mins {
- accelerate to 900   compensate lack of 90 GeV reset
- turn on low β (switch to 12 aperture)
- scrape beams

10 minutes overhead / 2 hour cycle

~ $\frac{7}{8}$ %

──────────────────────────────

Kickers
need ~ 250ns rise/fall to get best boxcar stacking.
  - have E17 Medium straight for proton shuttered Kicker. D48 p̄ bar harder but don't need shutter.
  - haven't looked at abort shutter. may need fast p̄ abort too.

Worries

- Long range beam-beam effects.
  $\frac{1}{r^2}$ force at each passing $\Rightarrow$

      dipole distorts double helix
      quad shifts tunes
      sext shifts ξ
           etc.

  these are intensity dependent effects
  and weak-strong may cause problems.
  (SSC study of $\bar{p}p \Rightarrow$ for 600-1200 bunches
  at 5×10^{32} need 15 mm separation.
  We have lower $\mathcal{L}$, fewer bunches and
  15 mm.)

- Different ~~tot-tune~~ parameters for each beam
  due to different closed orbits.
  e.g. tunes are different due to orbit differences
  through sextupoles. Similar "feed down" of
  multipoles exists for all multipoles.
  Most worrysome is "feed down" for skew multipoles
  - may need clever inventions for independent
  coupling adjustments for the 2 beams.
        (e.g. skew quads, shuttered skew quad
- ~~Depolarization Problems.~~

Conclusions:

$$\langle \mathcal{L} \rangle = 5 \times 10^{31} \quad (\text{not just } \mathcal{L}_{peak})$$

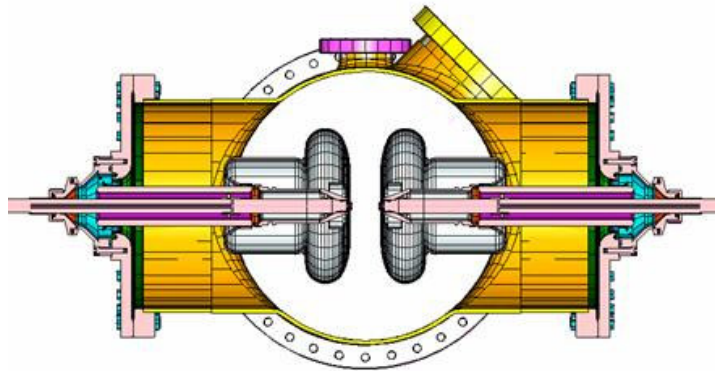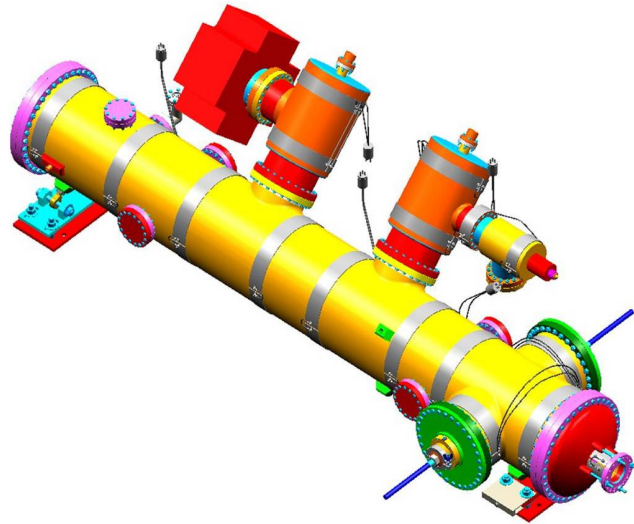looks good. There is a scheme without real technological extrapolations. (the Double Helix and consequences may be one — needs more work)

$$\text{Why not} > 5 \times 10^{31} \text{?}$$

Conditioning tests at MP-9

- **Tevatron Separator breakdown history**

- **Conditioning test facility at MP-9**

- **Separator R@D:**
    - **conditioning tests up to 180kV**
    - **hand/electro polish stainless steel plates**
    - **titanium plates**

- **Plans**

There are 22 beam separators in the Tevatron main ring

Fermi news:

… Tev separator sparked and kicked out the last bunch…

… C17 separator started sparking…

… TeV vertical separator sparked 3 times…

…. store 4078 quenched due to separator spark…

…. separator sparks caused loss of luminosity and then…

Electrode length – 101.25"

Electrode gap – 50 mm

Maximum voltages – up to 120 kV / plate)
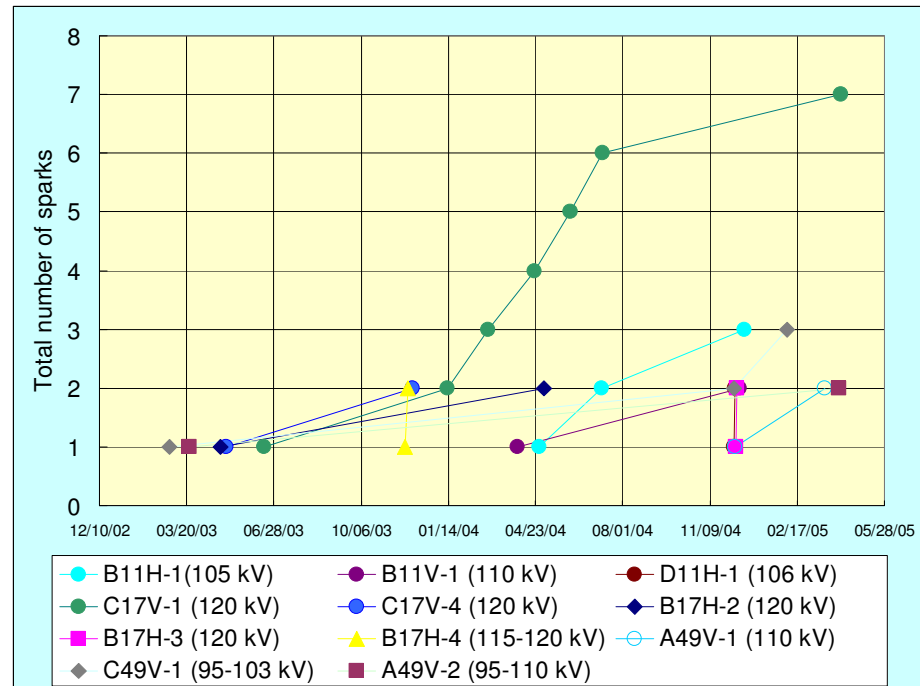
Conditioning Test Facility at MP-9

New factory (clean room, baking oven, conditioning cave) was constructed at MP-9 for building beam separators (BTeV project).

R&D is being done to improve separator performance and reliability.
Tests new electrode materials, conditioning procedure
Goals: 1 spark/year at 150 kV/plate (60 kV/cm)

Measuring scheme

TSP

Spark
Detector

Spark
Detector

Shunt
1 MOhm

Shunt
1 MOhm

Polarity

Positive Polarity

Negative Polarity

Polarity
Switch

HV ⊖

HV ⊕

Control Unit

DAQ
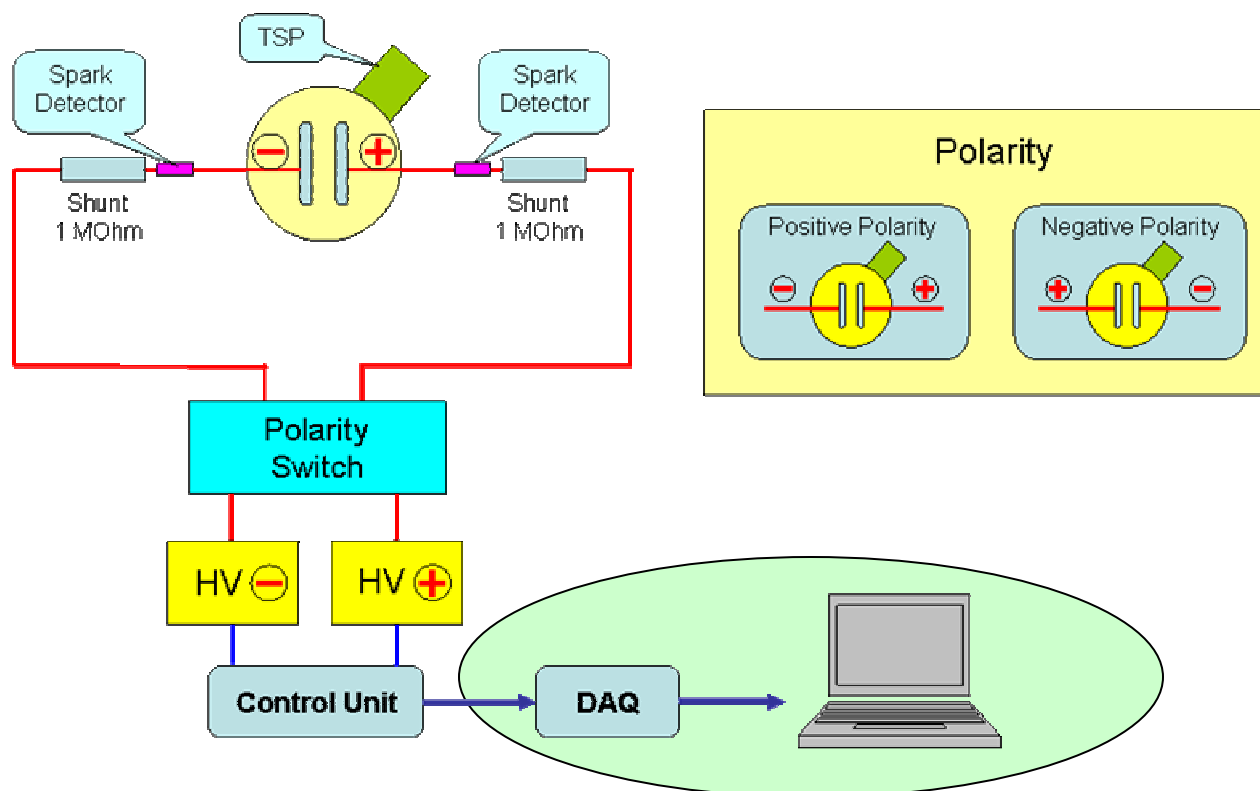
New Materials for Electrodes

Separator # 6 with Electro Polish Plates
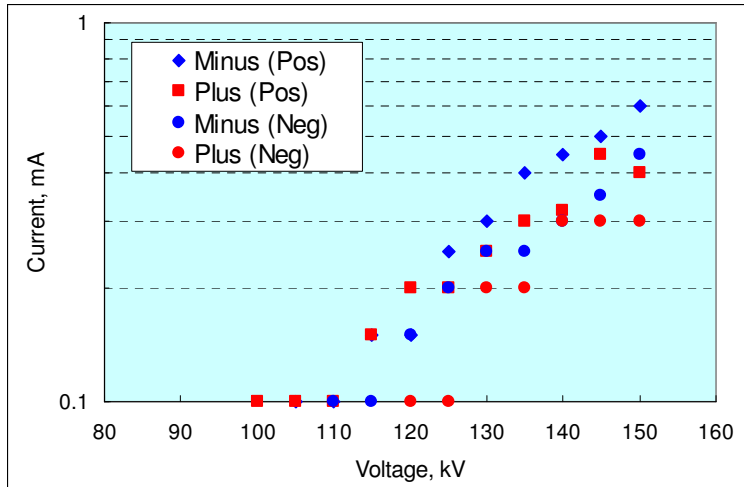
Current at 150 kV is about 0.5 µA at both polarities

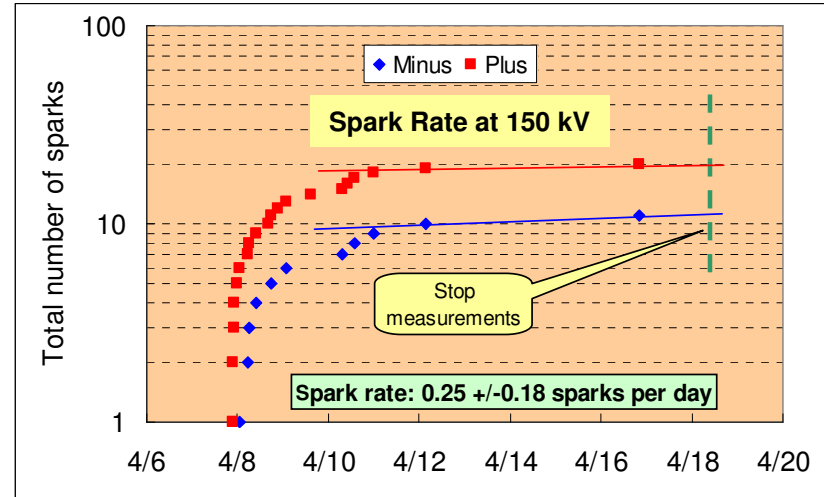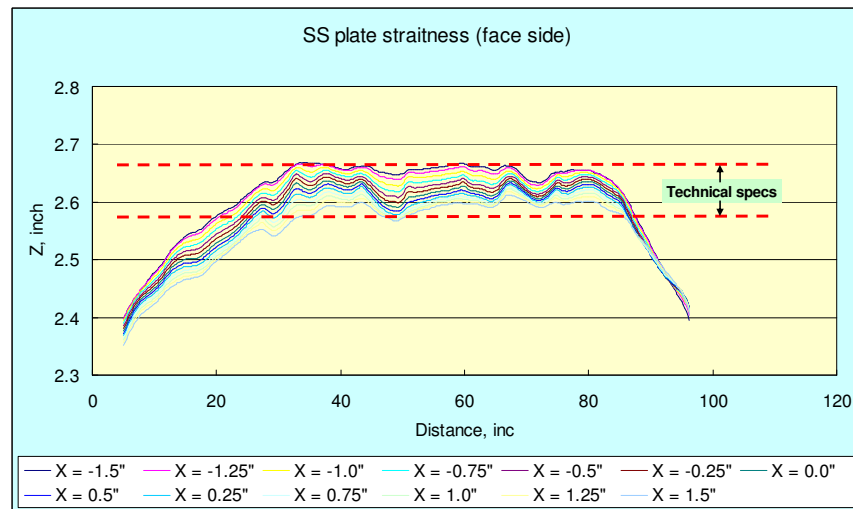Low spark rate ~ 0.25 spark/24 hours

Titanium Plates

Status of the Tevatron Low Beta and Separator Projects

K.P. Koepke

Fermi National Accelerator Laboratory*

P.O. Box 500

Batavia, Il 60510 USA

Abstract

Two low beta insertions and a set of electrostatic separators have been installed in the Tevatron. This gives the Tevatron two independently adjustable low beta insertions and the ability to separate the colliding beams everywhere except at the low beta collision points. The status of the installation will be summarized and the initial operating experience with the equipment will be reported.

1. INTRODUCTION

Two new low beta insertions [1] and 22 electrostatic separators [2] have been installed in the Tevatron. The old low beta insertion at the B0 interaction region of the Tevatron has been replaced and a second and essentially identical low beta insertion has been installed at D0. The D0 low beta insertion will serve the D0 detector which will come on line during the 1992 collider run scheduled after the new systems have been commissioned.

In the past, the Tevatron Collider has operated with a single low beta insertion [3] located at B0, the location of the Collider Detector Facility (CDF). This insertion functioned reliably but was not matched to the rest of the lattice. This mismatch introduced beta function and dispersion distortions to the rest of the Tevatron lattice that made it difficult to add additional low beta insertions to the Tevatron or to obtain uniform proton- antiproton beam separation with electrostatic separators.

The beta functions and dispersion of the new low beta insertions are completely matched to the lattice. This allows two or more insertions to operate simultaneously, coupled only through the tunes. Each low beta insertion adds approximately a half unit to the tunes of the lattice. The dispersion at the interaction point of the old low beta insertion was approximately 0.2 m. The dispersions at the interaction points of the new low beta insertions are approximately zero.

The low beta insertions increase the luminosity of the interaction regions. The luminosity of a proton-antiproton interaction point is given by the expression,

$$L = \frac{3\,\gamma\,f\,B\,N_p\,N_{\bar{p}}}{\beta^*\,(\varepsilon_p + \varepsilon_{\bar{p}})}\,F \qquad (1)$$

where γ is the relativistic factor of the protons and antiprotons, f is their revolution frequency, B is the number of proton (or antiproton) bunches, N_p and $N_{\bar{p}}$ are the number of protons and antiprotons per bunch respectively, F is a form factor that compensates for the longitudinal bunch length, ε_p and $\varepsilon_{\bar{p}}$ are the 95% normalized transverse emittances of the beams, and β^* is the value of the beta functions, assumed equal, at the interaction point. The low beta insertions increase the luminosity by lowering β^* from the nominal 70 m of a standard straight section down to .25 m.

The electrostatic separators separate the proton-antiproton closed orbits everywhere except at the B0 and D0 interaction points. This reduces the beam-beam tune shift experienced by the protons and antiprotons to a minimum by eliminating the unwanted beam crossings in the Tevatron. The antiproton beam-beam tune shift per beam crossing is given by the relation,

$$\Delta\nu = .00733\,N_p/\varepsilon_p \qquad (2)$$

where N_p is in units of 10^{10} and ε_p is in units of π mm-mr. Without separators, the total antiproton beam-beam tune shift [4] in the Tevatron for 12 crossings (6 proton bunches on 6 antiproton bunches) has reached a value of .025. This equals the available working space in the tune diagram bounded by resonances of 10th order or less. The separators will permit an increase in the luminosity of the two Tevatron interaction regions by permitting an increase in the proton phase space density (N_p/ε_p) and an increase in the number of beam bunches.
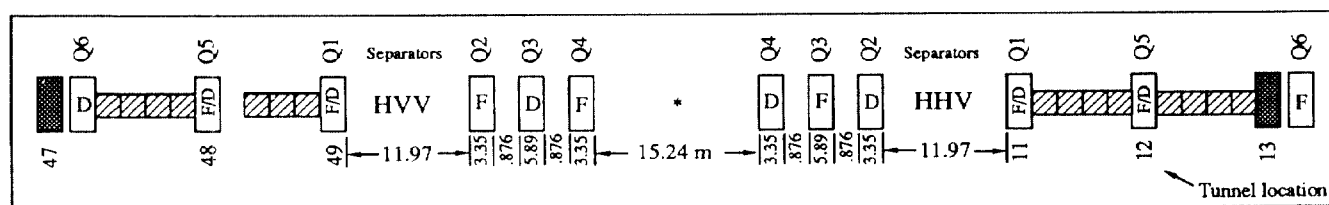

Figure 1. Central part of a low beta insertion. The magnetic lengths of the low beta quadrupoles and their relative placements are shown in meters. The filled elements are the remaining standard lattice dipoles and quadrupoles.

2. LOW BETA INSERTIONS

Each of the new low beta insertions consists of 18 quadrupoles designed and fabricated specifically for this application. The quadrupole parameters are given in Table 1. Two types of quadrupoles were utilized; a high gradient, high current 2-shell design for strong focusing at the center of the insertion, and a standard gradient, low current 1-shell design mounted at the start and end of the insertion for matching to the rest of the lattice. The low operating current of the 1-shell quadrupole is achieved by winding with 5-in-1 cable. Each cable contains 5 individually wrapped, oversized strands connected in series for an effective maximum current of 5 kA.

The B0 and D0 low beta insertions utilize interchangeable quadrupoles that have identical relative quadrupole placements. However, their physical supports and separate ancillary cryostat units reflect physical differences in the two collision halls. The center portion of an insertion is shown in Figure 1. The quadrupole pairs Q1 through Q5 are placed symmetrically relative to the center of the straight section. They are powered as focusing, defocusing pairs with equal gradients, equal effective lengths, and opposite gradient polarities. The remaining quadrupoles are mounted within special correction coil cryostats (called low beta "spools"). These "spools" are located downstream and adjacent to the normal lattice quadrupoles at the 43, 44, 46, 47, 13, 14, 16, and 17 locations of the standard lattice. These quadrupoles also function as focusing, defocusing pairs. However, as their placement is not exactly symmetric relative to the center of the insertion, they require slightly different currents in the upstream and downstream quadrupoles. A 15.24 m central region, equal to the region of the older B0 low beta insertion, has been left for the interaction region detector.

The low beta quadrupoles are powered independently of the Tevatron bus. This allows β^* to be programmed over a 1.7 m through .25 m range. The beta functions are antisymmetric relative to the center of the low beta insertion. The dispersion function is nonzero except at the interaction point. The dispersion could not be made uniformly zero within the low beta insertion because the insertion contains lattice dipoles. The dipoles could not be removed because of tunnel constraints.

The Tevatron alternates between periods of fixed target and collider operation. During fixed target operation, the D0 straight section contains the Tevatron's extraction septa. Therefore, the inner low beta components of the D0 low beta insertion are designed to be easily removable.

The low beta insertions are unpowered during fixed target operation as they add considerably to the heat load that the refrigerators have to remove. For example, each insertion adds 36 helium cooled power leads to the refrigeration system plus the cyclic heat load generated within the quadrupole coils. During collider operation, the cyclic heat load of the lattice magnets and low beta magnets is absent and the additional heat load of the low beta insertion is tolerable. During fixed target operation with

Table 1: Quadrupole parameters

	2-shell	1-shell
Number of quads per insertion	12	6
Peak gradient (T/cm)	1.4	0.58
Peak current (kA)	4.8	1.0
Q1 (T7) magnetic length (m)	1.4	.762
Q2 (T8)	3.35	.762
Q3 (T9)	5.59	.762
Q4	3.35	
Q5	1.4	
Coil inner diameter (cm)	7.5	7.5
Number of turns/pole inner	19	13
Number of turns/pole outer	28	
Strand diameter (size)(mm)	.528	1.09x1.76
Number of strands/cable	36	5*
Cable dim. w/o insulation(mm)	.897x9.78	1.09x8.8
Copper/superconductor ratio	1.5	1.5
NbTi short sample 5T,4.2K (A/mm^2)	3000	3000
* Each strand is insulated		

powered low beta components, the refrigerator satellites adjacent to the low beta insertions would have required added capacity. The exception to the not-powered rule are the Q2, Q3, and Q5 quadrupoles at B0, and the Q5 quadrupoles at D0. Their currents during fixed target operation are readjusted to mimic the function of the standard lattice quadrupoles that were removed to make place for the low beta insertion.

During collider operation, beam is injected into the Tevatron and accelerated to peak energy with β^* equal to 1.7 m. This lowers β_{max} on either side of the insertion to approximately 250 m, and reduces the probability of beam loss near the interaction region detectors during the time of the acceleration cycle when the beam is at its largest. The newly installed vertex detector at B0 is particularly sensitive to radiation damage. After the peak energy has been reached, β^* is reduced to increase the luminosity.

3. ELECTROSTATIC SEPARATORS

A 9 m long clear space has been left on both sides of the low beta insertion for electrostatic separators. The distribution of all the electrostatic separators within the Tevatron is shown in Figure 2. The horizontal and vertical separators are physically identical, differing only in their 90 degree relative orientation when installed. Each separator has a 3 m slot length, an electrode separation of 5 cm, and a nominal maximum operating field of 50 kV/cm. The electrode pairs are connected to separate power supply pairs that have opposite voltage polarities relative to a common ground. Up to four separators have been connected to a common power supply pair to obtain the required kick angle.

The separators have been made as strong as possible and are placed symmetrically and as close as possible to the interaction point. This separates the colliding proton-antiproton bunches before they reach the next beam crossing points on both sides of the interaction region. Beam crossings at small bunch separation are believed to be more harmful to the beam than head on crossings and may

ultimately limit the maximum number of bunches that are injected into the Tevatron.

The separators function as "3-bumps" in the vertical and horizontal planes to form separated orbits. The proton-antiproton bunches are on the unseparated closed orbit as they collide at B0 and D0. When the bunches exit the interaction region, the separators kick them off-axis vertically and horizontally. The bunches now oscillate around the unseparated orbit and the approximately 90 degree phase difference between the vertical and horizontal oscillations prevents any head-on crossings . The proton-antiproton displacements relative to the unseparated closed orbit are always equal but of opposite sign. Vertical and horizontal separators located between B0 and D0 are adjusted to bring the bunches back on the unseparated orbit as they cross the third set of vertical and horizontal separators before entering B0 and D0. The third set of separators is adjusted to cancel the orbit slopes present as the bunches enter the separators. This maintains the bunches on the unseparated orbit as they again cross B0 and D0 for another collision.

The acceleration sequence of the Tevatron collider is as follows: The proton bunches are first injected onto the unseparated Tevatron closed orbit. Then the horizontal separators at B11 and B17, and the vertical separators at C17 are turned on. These separators result in totally separated orbits for the protons and antiprotons with the proper orbit displacements at the antiproton injection septum magnet after the antiprotons are injected. The counter-rotating bunches are accelerated on these orbits and remain on them until the low beta insertions are adjusted to a lower β^*. Finally, the remaining separators are rapidly turned on to bring the protons and antiprotons into collision at the B0 and D0 interaction regions.

4. STATUS

All of the B0 low beta insertion, and all of the D0 low beta insertion except Q1 through Q4, were installed and commissioned prior to the 1991 fixed target run. The remaining D0 insertion quadrupoles were installed during the February 1992 shutdown after the completion of the fixed target run. The successful completion of the fixed target run indicates that the low beta insertions installed at B0 and D0 have not degraded the Tevatron's fixed target capability.

Approximately half of the electrostatic separators had been installed and commissioned prior to the February 1992 shutdown. The rest were installed during the shutdown. Six of the separators were powered during the fixed target run to measure their tunnel sparking rate in the presence of beam. The separators were tested "parasitically" by forming local orbit bumps with the separators and adjacent lattice correction dipoles. At 50 kV/cm, a single spark occurred during a full week of operation.

The performance of the B0 low beta insertion in collider mode was tested with protons immediately after its installation down to a β^* of .5 m. Prior to the February
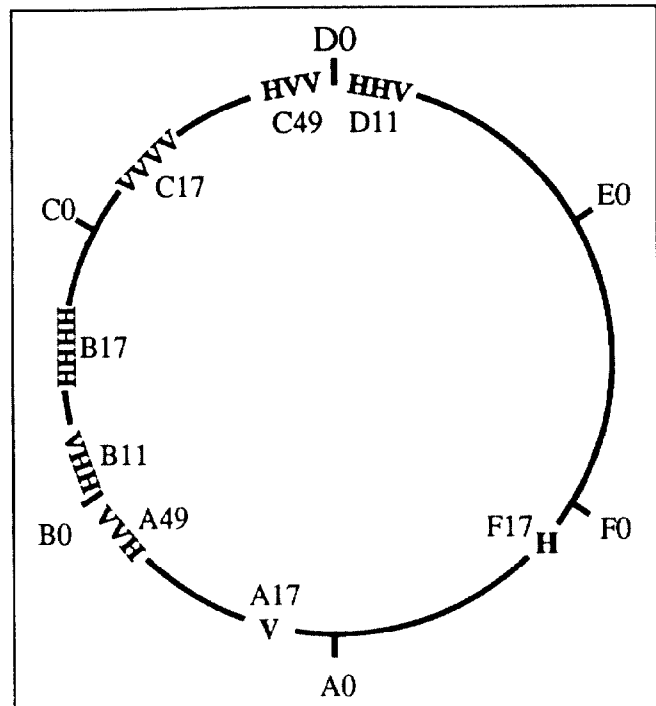

Figure 2. Tunnel placement of the electrostatic separators.

1992 shutdown, it was further tested with protons, antiprotons, and separators as follows: Protons and antiprotons were injected into the Tevatron and accelerated to full energy on separate closed orbits; the B0 low beta insertion was adjusted to a β^* of .5 m; and the separators were reprogrammed to bring the beams into collision at B0.

The first test of the whole system will be the collider run scheduled for this year. At this time, the D0 low beta insertion and the remaining electrostatic separators are still undergoing electrical tests without beam. The next phase of commissioning will include a short period of beam studies and tuning, followed by the first collider run with separated orbits and two low beta insertions in the Tevatron.

5. REFERENCES

[1] A.D. McInturff, J. Carson, T. Collins, K. Koepke, E. Malamud, P. Mantsch, R. Niemann, and A. Riddiford, "The Fermilab Collider D0 Low Beta System", EPAC 1988, pp. 1264-1266

[2] E. Malamud, "Tevatron Orbit Separator Design", Snowmass, 1988

[3] D.E. Johnson, "The B0 Low-Beta Insertion Design for the Tevatron", IEEE Transactions on Nuclear Science, 1985, pp. 1672-1674

[4] S. Holmes, "Achieving High Luminosity in the Fermilab Tevatron", IEEE Proceedings of the 1991 Particle Accelerator Conference, May 1991, pp. 2896-2900

BEAM LOSS HANDLING AT TEVATRON: SIMULATIONS AND IMPLEMENTATIONS

A.I. Drozdin and N.V. Mokhov*, Fermilab, P.O. Box 500, Batavia, IL 60510 USA

Abstract

Summary of studies is presented towards minimization of beam loss in the critical locations at the Fermilab Tevatron to reduce background rates in the collider detectors and to protect machine components. Based on detailed Monte-Carlo simulations, measures have been proposed and incorporated in the machine to reduce accelerator-related instantaneous and residual background levels in the DØ and CDF detectors. Recent measurements are in good agreement with the predictions. A re-alignment of the electrostatic deflector and the Lambertson magnet and the addition of shielding in the AØ straight section has resulted in reduction of beam induced energy deposition in the superconducting magnets, which allowed an increase in the extracted beam intensity. Using the same simulation technique, it has been calculated that the total beam of 10^{13} protons can be removed from the Tevatron at the end of the store, leaving the antiproton beam in the machine for recycling. Using the EØ collimator with attached scattering targets, this process will require about 100 seconds to keep the power deposition in the superconducting magnets below the quench level.

1 INTRODUCTION

Tevatron is the world's first superconducting and most powerful hadron collider. Enormous efforts at Fermilab, reliably provided 900×900 GeV $p\overline{p}$ collisions with the peak luminosity up to 2.5×10^{31} cm^{-2} s^{-1}, recently resulted in the discovery of the top quark, among many other important achievements. The current fixed target run, begun in May 1996, exhibits the impressive performance of both the machine and experiments. At the same time, work progresses to upgrade the accelerator and detectors into even more powerful research tools [1]. The high performance of Tevatron both in the fixed target and collider modes is achievable only with a dedicated beam cleaning system embedded in the lattice [2, 3, 4].

2 BEAM LOSS HANDLING

In the Tevatron, as in any other accelerator, the creation of a beam halo is unavoidable: proton (antiproton) scattering in the IPs, in beam-gas interactions and on the limiting apertures, the diffusion of particles due to various nonlinear phenomena out of the beam-core, as well as various hardware and software errors – all result in emittance growth and eventually in beam loss in the lattice [2, 5, 6].

This causes irradiation of conventional and superconducting (SC) components of the machine, an increase of background rates in the detectors, possible radiation damage, quench, overheating of equipment and even a total destruction of some units. A very reliable multi-component beam collimation system is the main way to handle beam loss and is mandatory at any SC accelerator, providing [4, 5, 6]:

- reduction of beam loss in the vicinity of IPs to sustain favorable experimental conditions;
- minimization of radiation impact on personnel and environment by localizing beam loss in the predetermined regions and using appropriate shielding in these regions;
- protection of accelerator components against irradiation caused by operational beam loss and enhancement of reliability of the machine;
- prevention of quenching of SC magnets and protection of other machine components from unpredictable abort and injection kicker prefires/misfires and unsynchronized abort.

At the early Tevatron days the first collimation system was designed [2] on the basis of the MARS/STRUCT [7, 8] full-scale simulations of beam loss formation in the machine. The optimized system, consisted of primary and secondary collimators about 1 m long each, was installed in the Tevatron which immediately made it possible to raise by a factor of 5 the efficiency of fast resonant extraction system and intensity of the extracted 800 GeV proton beam. The data on beam loss rates and on their dependence on the collimator jaw positions were in an excellent agreement with the calculational predictions.

Later, we have refined the idea of a primary-secondary collimator set and shown that this is the only way to use such a system in the TeV region with a length of a primary collimator going down to a fraction of the radiation length. The whole system should consist then of a primary 'thin scattering target', followed immediately by 'a scraper' with a few 'secondary collimators' in the appropriate locations in the lattice [5, 6]. The purpose of a thin target is to increase amplitude of the betatron oscillations of the halo particles and thus to increase their impact parameter on the scraper face on the next turns. This results in a significant decrease of the outscattered proton yield and total beam loss in the accelerator, scraper jaws overheating and mitigating requirements to scraper alignment. Besides that, the scraper efficiency becomes independent of accelerator tuning, there is only one drastic restriction of accelerator aperture and only the scraper region needs heavy shielding and probably a dogleg structure. The method would give

133

an order of magnitude in beam loss reduction at multi-TeV machines, but even at the Tevatron we have got a noticeable effect. Recently the existing scraper at AØ was replaced with a new one with two 2.5 mm thick L-shaped tungsten targets with 0.3 mm offset relative to the beam surface on the either end of the scraper (to eliminate the misalignment problem), resulting in reduction of beam loss rate upstream of both collider detectors [3]. A few other recent studies are described in the following sections.

3 FORWARD PROTON DETECTOR

The detector [9] consists of four Roman Pot units placed in the DØ straight section upstream and downstream of the separators, and of three units at the C48 location. Each unit consists of two square 2×2 cm^2 detectors placed from both sides of the closed orbit.

Particle background in the Roman pot detectors is originated in proton and antiproton interactions with the primary and secondary collimators. The primary collimators are positioned at 5σ while secondary ones at 8σ. The Roman pot detectors are at $8\sigma_x$ for proton beam and $9.4\sigma_x$ for antiprotons. Moreover, antiproton intensity intercepted by the collimation system is 3.6 times lower compared to the proton intensity. Therefore, antiproton background in the Roman pots amounts only 2% of the total background, and backgrounds in the DØ detector due to Roman pots on the proton side about two orders of magnitude higher compared to the antiproton side.

Total background hit rates in Roman pots are (2.3-3.3)$\times 10^6$ p/s for detectors at $8\sigma_x$ and (0.87-1.09)$\times 10^6$ p/s for detectors at $9\sigma_x$, i. e. the rates are three times lower for the detectors at larger distance from the closed orbit. Beam loss distributions in Tevatron with the Roman pot detectors at $8\sigma_x$ are presented in Fig. 1.
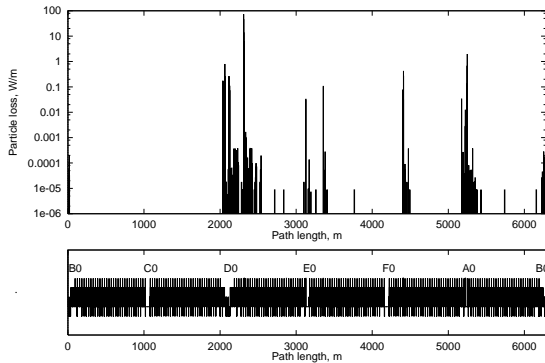

Figure 1: Beam loss distributions in Tevatron for D17 collimation with Roman pots at $8\sigma_x$.

4 FAST RESONANT EXTRACTION

Our recent simulations have shown that with the appropriate collimation, additional shielding in AØ and electrostatic deflector and Lambertson magnet realignment, one could reduce beam loss rates in Tevatron and increase the extracted intensity without quenches. It was found that in a

narrow region of resonance phases used for extraction, the angle of the Lambertson magnet alignment depends mostly on the septa position, not on the resonance phase. This angle is equal to x'=-0.330 mrad for the septa at 20 mm from the beam orbit. Any misalignment can drastically increase the effective septum thickness and thus beam loss.
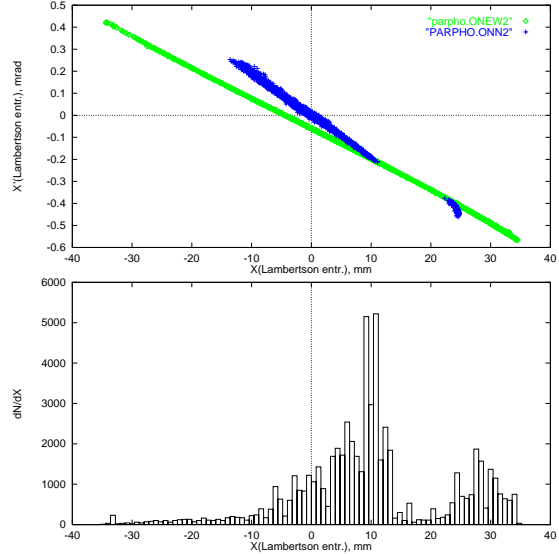

Figure 2: Fast extraction phase space at the AØ Lambertson magnet entrance. Top – extracted beam (black crosses) and protons outscattered from the DØ deflector (grey squares). Bottom – transverse distribution of outscattered protons.

Proton distributions at AØ are shown in Fig. 2 with proton beam kicked by the DØ electrostatic septum. Protons outscattered from the septum wires are intersepted by the Tevatron collimators. The EØ straight section is a very convenient place for the absorption of scattered protons, but unfortunately, there is no collimator in this location. It was found that the antiproton injection Lambertson magnet can be used as a collimator with particles catched by the normal conducting magnet yoke. Fast resonant extraction related beam losses (in SC magnets only) with and without collimation are presented in Fig. 3. Collimation system reduces beam losses in the superconducting magnets downstream of D17 by one order of magnitude. The DØ collimator right after the septum, catching the low-energy debries from the wires, unfortunately doesn't protect the DØ - D17 region.

Calculations show that a 1 m long collimator (r_{in}=15 mm) upstream of the extraction line superconducting skew dipoles will protect them from the secondaries produced in the Lambertson magnet. Similar collimator with a round aperture of r_{in}=20 mm upstream of the first and second quadrupoles will protect them and other ring superconducting magnets.

5 PROTON BEAM REMOVAL

The upgrade plan requires to remove proton beam from Tevatron before the deceleration leaving antiproton beam for recycling. There are two main concerns with the intense
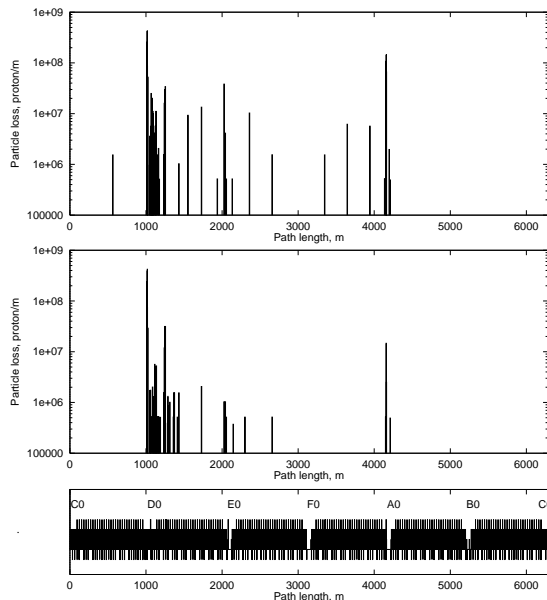
Figure 3: Fast resonant extraction losses without collimation (top), and with DØ , D17, F17, F49, AØ collimators and Lambertson magnet at EØ (bottom).

beam fast removal: superconducting magnet quenches caused by secondaries from a collimator and a target-collimator assembly overheating. A quench level of the Tevatron magnets at 1 TeV is about 3×10^8 p/m/s. This corresponds to about 50 W/m. A good practice is to keep a heat load to cryogenics below ~ 1.5 W/m, or 1×10^7 p/m/s.

With the Main Injector, the EØ straight section becomes free of the magnets used for the beam injection into the Tevatron. With the first 15 m of EØ straight section reserved for RF, the rest 35 m can be successfully arranged for the proton beam removal (Fig. 4). Four DØ conventional bump-magnets are supposed to be used for the EØ dog-leg to protect the Tevatron magnets against neutral and low-energy charged particles out of a primary collimator. Two 1.5 m long L-shaped secondary collimators placed at 10σ downstream of the dog-leg at the entrance to the cold region intercept most secondaries. With such a system, the maximum beam loss in the Tevatron SC magnets is estimated to be 1.4 W/m. Moreover, the calculations show that it allows to get rid of other secondary collimators in the machine and, what is remarkable, reduce the beam loss level in the DØ - D17 region by about a factor of four.

The EØ target heating is a serious problem for short spills. An instantaneous target temperature rise is 10000°C. The target-collimator assembly cooling tremendously decreases this temperature. With this, for a 10 msec spill a stainless steel collimator edge is heated up to 1600°C, but already for a 1 sec spill, $\Delta T_{max} = 40°C$, only. So, the target-scraper assembly overheating seams is not a restriction for the proton beam removal from Tevatron.

Calculations show that total beam intensity of 10^{13} can be removed from Tevatron during 100 s using EØ collimator. During the January 1997 experimental studies, proton
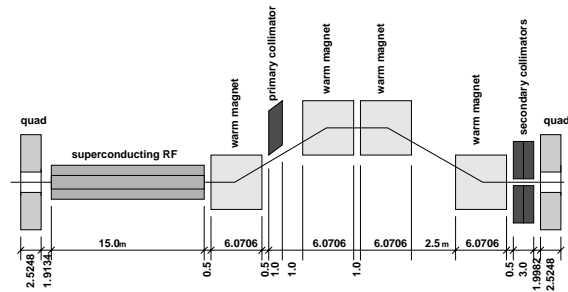

Figure 4: Dog-leg scheme for proton beam removal at EØ straight section.

beam was removed from Tevatron without problem until a SC magnet quench happened at the rate of 0.36×10^{11} p/s. This is three times below of that was expected, what is easily explained by absence of a scattering target in the collimator and possible closed orbit displacement. Moreover, analysis of the spill at beam removal has shown peaks of losses at frequency of 1, 4.6, 13.9, 21, 37, 73 and 90 Hz, which are understood from the Main Ring and Central Helium Liquefier performance and the beam position oscillations with synchrotron frequency. The experiment has shown that a feed-back system from the Beam Loss Monitors to the dipole correctors used for the beam displacement is necessary. This system would provide rectangular spill shape and eliminate low-frequency peaks (1-37 Hz).

6 REFERENCES

[1] D.A. Finley, J. Marriner and N.V. Mokhov, 'Tevatron Status and Future Plans', Fermilab–Conf–96/408, 1996.

[2] A.I. Drozhdin, M. Harrison and N.V. Mokhov, 'Study of Beam Losses During Fast Extraction of 800 GeV Protons from the Tevatron', Fermilab FN-418, 1985.

[3] J. Butler, D. Denisov, T. Diehl, A. Drozhdin, N. Mokhov and D. Wood, 'Reduction of Tevatron and Main Ring Induced Backgrounds in the DØ Detector', Fermilab–FN–629, 1995.

[4] N.V. Mokhov, 'Optimization of the Radiation Environment at the Tevatron', in Proc. of the Second Workshop on Simulating Accelerator Radiation Environments, CERN, October 1995, CERN/TIS-RP/97-05, 1997.

[5] M. Maslov, N. Mokhov and I. Yazynin, 'The SSC Beam Scraper System', SSCL-484, 1991.

[6] A. Drozhdin, N. Mokhov, R. Soundranayagam and J. Tompkins, 'Toward Design of the Collider Beam Collimation System', SSCL-Preprint-555, 1994.

[7] N. V. Mokhov, 'The MARS Code System User's Guide, Version 13(95)', Fermilab–FN–628, 1995.

[8] I. Baishev, A. Drozhdin and N. Mokhov, 'STRUCT Program User's Reference Manual', SSCL–MAN–0034, 1994.

[9] A. Brandt, A. Drozhdin, N. Mokhov et al., 'Proposal for Forward Proton Detector at DØ' Fermilab, October 1996.

LONG-TERM SIMULATION OF BEAM-BEAM EFFECTS IN THE TEVATRON AT COLLISION ENERGY

A. Kabel[*], Y. Cai, SLAC, Stanford, CA 94025, USA
T. Sen, FNAL, Batavia, IL 60510, USA

Abstract

The beam-beam effect is a significant source of non-linearities in the Tevatron. We have developed a code which allows us to estimate its contribution to the finite lifetime of the anti-proton beam, both at collision and injection energy, by tracking realistic particle distribution for a high number of terms and extrapolating from the particle loss rate. We describe the physical modeling underlying the code and give benchmarking results.

INTRODUCTION

In its current operating mode, the Tevatron operates with 36+36 (anti-)proton bunches circulating in the same beampipe on separated helices and being brought to collision in two interaction points, B0 and D0 at an collision energy of 980GeV.

Thus, each bunch will experience 2 design and 70 parasitic collision with an antagonist bunch. The pattern of parasitic crossings experienced by the weak bunch will depend on the cogging stage and the number of the bunch in its train; a three-fold symmetry introduces equivalence classes of bunches, reducing the number of discernible bunches to 12.

In the injection stage with an energy of 150GeV, the helices are completely separated, leading to 72 parasitic collisions. In both cases, the beam-beam effect will exert strongly non-linear forces on the anti-proton bunch, possibly leading to particle loss due to diffusion or incoherent resonances. In the past, we have been able to predict particle loss rates and extrapolate lifetime signatures for different operating parameters with long-term tracking studies using a crude approximation of the lattice dynamics of the Tevatron. In this paper, we study a more careful implementation aimed at preserving the more important non-linear effects of the lattice, in particular chromaticity, while retaining the high tracking speeds necessary. We can not expect absolutely to predict beam lifetimes (at injection and collision, the typical timescales are $10h$ and $100h$; requiring about 10^{12} and 10^{14} particles·turns simulation effort, resp.), but attempt to establish signatures of beam loss rates for different operational parameters.

PHYSICAL MODELLING

The goal of our tracking studies is to obtain insight into beam loss rates and lifetimes by tracking macro-particles

---

for very long times and recording their amplitude vs. time behavior, thus going beyond the more conventional dynamic aperture calculation which only provide a limited insight about the machine behavior.

Clearly, a full simulation of the machine–full number of particles, full lattice, full machine-time simulation–is beyond today's computational resources. We have to restrict ourselves to

- a simplified model of the lattice. While retaining all beam-beam interactions exactly, the rest of the lattice can be lumped together as either linear elements; chromatic elements (see below), or can be treated element-by-element, where multipoles are handled to the required order, other elements symplectically with up-to-cubic hamiltonians.

- a restriction of the number of turns and the number of particles; the maximum $N_{Turns}N_{Particles}$ is limited by the speed and number of CPUs available; a rough estimates shows that we require $N_{Turns}N_{Particles} \geq 10^{10}$ to predict lifetimes in the range of hours.

- the restriction of the number of turns forces us to extrapolate from the loss rate vs. turn number to its long term behavior. Solutions for the diffusion equation with absorbing boundary conditions (provided by the scraping aperture) behave as $\propto e^{-\sqrt{t/T}}$ and $\propto e^{-t/T}$ for small and large apertures, resp.; we use Ts obtained by a fitting to both asymptotic behaviors to characterize loss rates.

THE TRACKING CODE dumbbb

To address the issues laid out in the previous sections, a code, 'dumbbb', was developed. Great care was taken to yield maximum speed for raw tracking while retaining the flexibility of a general-purpose tracking code; i. e., easy set-up and manipulation of beamlines and parameters as well as flexibility in the choice of accuracy of the physical model and the resulting speed trade-off.

The structure of the code and the programming techniques used as well as a beam dynamics C++ library used as a programming environment are described in more detail in [5].

Lattice Manipulation

dumbbb will read a MAD 8.x conformant input file. As the MAD syntax seems not to be formally defined, the

---

* akabel@stanford.edu

parser is restricted to the well-defined subset of files generated by MAD's `SAVE` command.

The read file is converted to an internal representation, allowing for manipulation of elements and beamlines. In particular, a MAD definition can be expanded into a flat lists of beamline elements; flat lists, in turn, can be subject to insertions at arbitrary longitudinal positions, including within elements, which are split in two sections. This is used for inserting beam-beam elements at positions according to the currently examined bunch and cogging stage.

Elements

The flat list of elements acts as a 'class factory' for tracking elements proper. Each MAD element will generate a finite number of tracking elements, acting on particles' phase space vectors. The currently implemented elements and their implementation methods are:

- *Drift Spaces.* Either linear or first-order chromatic.

- *Quadrupoles.* Either linear or first-order chromatic. First-order chromaticity is implemented either by the exact solution of the 3rd-order Hamiltonian or by a sequence of thick-lens matrices and chromatic thin-lens kicks.

- *Sector Bends.* Either linear or first-order chromatic. Chromaticity is implemented as a sequence of thick-lens matrices and kicks according to the 3rd-order Hamiltonian.

- *Multipoles, RF Cavities, Electrostatic Separators* Implemented by a sequence of, possibly chromatic, drift spaces and thin-lens kicks.

- *Beam-Beam Elements, Tune Prints, Apertures, Counters.* See below.

Lumping and Optimization

The generated beamline and its elements can act either on raw floating-point phasespace vectors x or on differential-algebraic (DA) objects $x+\alpha_1 dx+\alpha_2 dx \vee dx+ \ldots$. At program startup, the closed orbits of both rings are determined (by Newton iteration) and differential-algebraic maps around it are constructed.

We then find the (3 each) eigendistributions' correlation matrices of the proton beam, use the emittances to construct beam matrices which, together with the orbit offsets with respect to the anti-proton orbit, are used to construct beam-beam elements at the 72 crossing points. Strictly speaking, this procedure should be iterated until convergent.

The interjacent elements can then be lumped together in a symplectic fashion, either by using a chromatic map (see below) or just a linear map. If no lumping is used, an optimization steps joins elements whose adjacent maps can be simplified, e.g., a sequence of two drift spaces, linear transfer elements, or thin-lens multipoles.

Using the full Tevatron lattice as of March, 2005, which, in our representation, comprises 12902 tracking elements, we obtain the tracking speeds given in 1. It should be noted that, given the estimated turn number from above, tracking element-by-element to obtain absolute lifetimes is not without the realm of the possible.

Table 1: `dumbbb` Tracking Speeds for Different Physical Models (on a 1.8GHz Xeon Processor

Model	Speed[turns/s]
200 Sextupoles + Chroma lumping	5700
9 6D slices + 70 4D parasitics	6200
+ 200 Sextupoles + Chroma lumping	3200
+ elment-by-element	610

Code Validation

We have carefully checked the validity of the tracking part of our code by comparing to established tools such as MAD 8.x. Optical functions on the zero orbit generally agree to CPU precision, on the helices, deviations of 10^{-5} can be observed, which can be traced back to the thin-lens approximation for the electrostatic separator in `dumbbb`.

Element-by-element tune prints (calculated by the Laskar method in `dumbbb`) show excellent agreement. Symplecticity of all element and lump maps is checked at program startup by tracking DA vectors; usually, the quantity $\sqrt{\sum_{ik}(M^\top JM - J)^2_{ik}} < 10^{-12}$.

A Symplectic Prescription for Chromatic Lumping

One of the dilemmas of high-order 'lumped' tracking is the non-symplecticity of a truncated power series expansions of a section map. This can be remedied by very high-order expansion, which is computationally expensive, or by any of a number of symplectification approaches.

For the problem at hand, chromatic effects seem to be of significant importance. When handling sextupoles in dispersive sections correctly, the chromaticity of the interjacent section also has to be implemented correctly to obtain the correct net chromaticity.

This can be achieved by writing the total map of a section as $\tilde{M} = M(1 - p_t G) + O(p_t^2) = Me^{-p_t G} + O(p_t^2)$, where M is the linear part of the map and G is a symplectic generator acting on the transverse subspace; it is obtained by evaluating the third-order map around the dispersion orbit. $e^{-p_t G}$ is symplectic by construction. By writing $H = -\frac{1}{2}JG$ and expressing H in an eigenbasis of G, the Hamiltonian reduces to any of three forms:

- $H = \alpha pq$, a rescaling operation

- $H = \frac{\beta}{2}(p^2 + q^2)$, a harmonic oscillator

- $H = \frac{\gamma}{2}(p^2-q^2+P^2-Q^2)+\delta(qP-Pq)$, an isotropic repulsive oscillator in a rotating frame of reference.

All these case can readily be evaluated either in closed form or as a sequence of 3 thin-lens kicks by determining the eigenvectors of JG and constructing a canonical basis in which it has harmonic oscillator form, reducing the problem to at most two quadrupole transformations.

Beam-Beam Effects

At present, the Tevatron is operated in the weak-strong regime of the beam-beam interaction. Assuming gaussian distributions, the effect on the antiproton bunch can then be calculated using the Bassetti-Erskine formula[3], which involves the evaluation of the complex error function.

While not the dominant part of CPU time for some of the more extensive beamline models, care was taken to find an efficient implementation. We benchmarked several numeric implementation and found the prescrition given in [4] to be fastest. Other approaches have been used in similar codes, such as Pade approximations and grid interpolations.

When $\beta_{x,y} \leq c\sigma_t$, the hourglass effect becomes important. We then have to slice the strong bunch and to include the full 6d dynamics of the weak bunch; the symplectic prescription used is given in [2]. We use several optimized functions, distinuishing the cases of

- Four-dimensional:
    - Coupling: tilted beam
    - No coupling: upright beam
- Six-dimensional:
    - Coupling: slice with position-dependent tilt
    - Coupling: beam with constant tilt
    - No coupling: upright beam

Weak Bunch Population

Lifetime calculations are based on particle migration rates across a boundary in configuration space. It is safe to assume that, for realistic distances of that boundary, most of the particles in that bunch will never cross that boundary within the simulated time; these stable particles will be close (in action space) to the closed orbit. A previous version of dumbbb consequently provided a 'de-coring' option, restricting bunch population to particles far (in action space) away from the closed orbit. Because of the high dimensionality of phasespace, the action radius of the omitted core has to be chosen quite large to result in an appreciable reduction of the particle number. This is unsatisfactory, however, as for high actions the deformation of surfaces of equal action due to the nonlinear dynamics becomes significant. The present version of dumbbb thus uses a weighted-macroparticle approach: The weak bunch is represented by particles equidistributed in radial and angular space in six-dimensional spherical coordinates; particles carry a
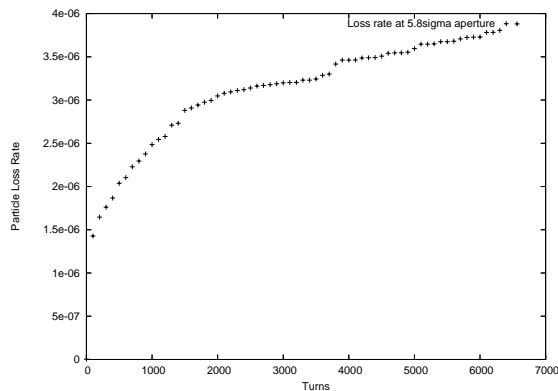

Figure 1: Typical Particle Loss Rate from Simulation Run

gaussian weight $\exp -r^2/2r^5 \mathrm{d}r \mathrm{d}\mathrm{d}\vartheta_4 \sin^4 \vartheta_1 \ldots \vartheta_5$. The cutoff radius of the distribution can be chosen freely. The radial and angular distribution is generated from an unique integer particle tag by means of a Halton pseudorandom sequence over the first 6 primes, thus reducing charge distribution noise and facilitating parallelization and reproducibility of simulation runs. It should be noted that, by weighting particles and recording their migration rates, post mortem emittance parameter scans for loss rates are possible by re-assigning weights according to different emittances.

Simulation Runs

We have ported the code to the DOE's NERSC facility SP computers and performed runs on 256 nodes each, varying chromaticity in steps of 5 from 0 to 20. An evaluation of the results will be the subject of a forthcoming paper. A typical particle loss rate is shown in figure (chromaticity 5, aperture 5.8σ).

ACKNOWLEDGMENTS

REFERENCES

[1] A. Kabel, Y. Cai, B. Erdelyi, T. Sen, M. Xiao, Proceedings of the 2003 IEEE Particle Accelerator Conference (2003)

[2] K. Hirata, H, Moshammer, F Ruggiero, Part. Acc. **40**,205 (1993)

[3] M. Bassetti, G Erskine, CERN ISR TH80-06 (1980)

[4] F. Matta and A. Reichel, Math. Comp. **25**, 339 (1971)

[5] A. Kabel, A C++ Framework for High-Speed, Long-Term Particle Trackign Studies, This Conference.

IMPROVING THE TEVATRON COLLISION HELIX*

R. S. Moore, Y. Alexahin, J. Johnstone, T. Sen

Fermi National Accelerator Laboratory, Batavia, IL 60510, U.S.A.

Abstract

In the Tevatron, protons and antiprotons circulate in a single beam pipe, so electrostatic separators are used to create helical orbits that keep the two beams separated except at the two interaction points (IP). Increasing the separation outside of the IPs is desirable in order to decrease long range beam-beam effects during high energy physics (HEP) stores. We can increase separation by running the separators at higher gradients or by installing additional separators. We are pursuing both strategies in parallel. Here, we describe Tevatron operation with higher separator gradients and with new separators installed during a recent shutdown. We also describe possible future installations.

INTRODUCTION

The Tevatron provides collisions of 980 GeV protons and antiprotons (36 bunches each) at the two IPs, denoted B0 and D0. The bunches are grouped in three symmetric trains of 12 bunches each. The bunches are separated by 396 ns (21 buckets) within the trains. Gaps between the trains are used for injecting antiprotons and for ramping up the extraction kickers when aborting beam. Typical beam parameters for recent high-energy physics stores are given in Table 1. Additional information on the Fermilab accelerator complex can be found in [1].

Since the two beams circulate within a single beam pipe in the Tevatron, 24 electrostatic separators are used to separate them around the ring, except the IPs where head-on collisions are desired for HEP stores. The electrostatic separators comprise two 100 inch stainless steel, parallel plate electrodes separated by a 5 cm gap through which the beams pass. Each electrode is connected to its own power supply. The maximum design separator gradient for HEP operation was 40 kV/cm, but we have been testing the use of the higher gradients to provide additional beam separation.

For colliding beam operation, the separators are grouped to form closed three-bumps in each plane (horizontal and vertical) in the so-called short (B0→D0) and long (D0→B0) arcs between the two IPs. This arrangement allows control of beam-crossing offsets and angles in each plane at the two IPs independently. Figure 1 shows the separation between the two beams at all parasitic crossing points around the Tevatron. The separation s is defined as:

$$s = \sqrt{\left(d_x/\sigma_x\right)^2 + \left(d_y/\sigma_y\right)^2} \,, \qquad (1)$$

where d_x, d_y are the horizontal, vertical distances between the protons and antiprotons, and σ_x, σ_y are the horizontal, vertical beam size assuming 95% transverse emittances of 20 π mm mrad. The first parasitic crossings, located 59 m away from the IPs, have the smallest separations, so they are the dominant contributors to long-range beam-beam effects during HEP stores. Improving the collision helix entails increasing the beam separation to help mitigate detrimental long-range beam-beam effects [2-4].

Table 1: Typical beam parameters at the beginning of recent Tevatron HEP stores.

Proton Intensity / Bunch	230-240 E9
Proton Transverse Emittance (95%)	16-18 π mm mrad
Proton Bunch Length	1.58-1.68 ns
Pbar Intensity / Bunch	25-75 E9
Pbar Transverse Emittance (95%)	9-15 π mm mrad
Pbar Bunch Length	1.52-1.62 ns

ADDITIONAL SEPARATORS

Employing additional separators is one way to provide additional separation between the protons and antiprotons. However, available warm space at appropriate betatron phase advances is rather limited, and some spare separators must be retained for use in the event of a failure. We have developed a proposal to install five additional separators at four locations: two vertical separators at D17 (long arc), one horizontal at A17 (long arc), as well as one horizontal and one vertical at B48 (short arc). These additional separators help increase separation in the specified plane only for the arc in which they are placed. The new separators combine with the old to form closed horizontal or vertical four-bumps within each arc. Consequently, the new separators do not need to be installed all at once in order to gain increased separation. As an example, the D17 separators were installed during the fall 2004 shutdown, and they have been used for HEP stores since then.

Figure 1 demonstrates how the beam separation benefits from the additional separators. The separations at
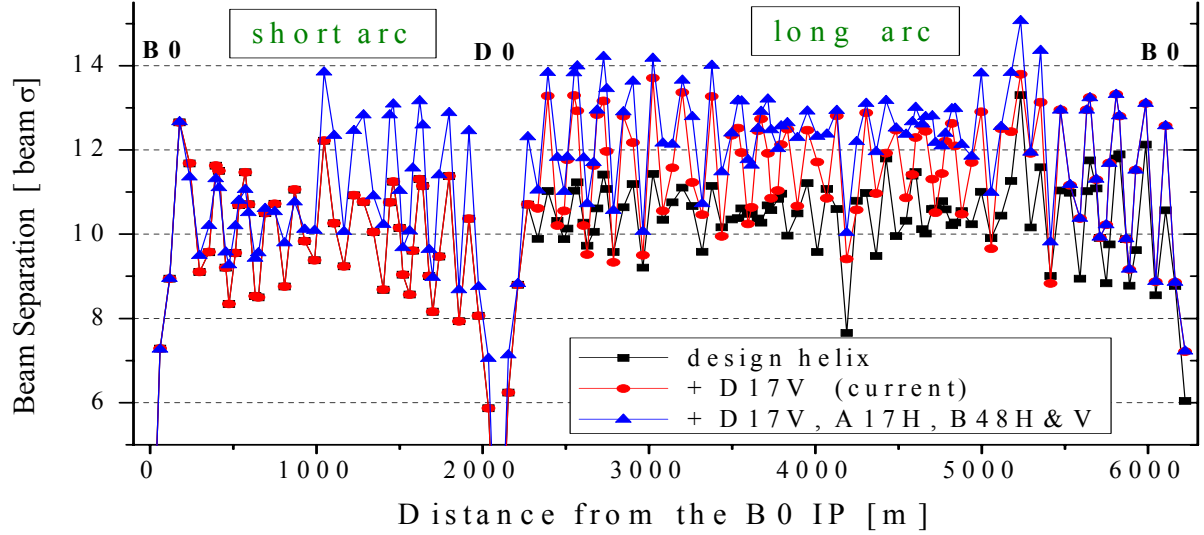

Figure 1: Separation between protons and antiprotons at all parasitic crossings for the design separator configuration (black squares), with the addition of vertical separators at the D17 location (red circles), and with all proposed additional separators (blue triangles).

the first parasitic crossings can be increased by approximately 1σ (≈15%), while the *average* separation in the arcs increases by a similar amount. In addition, the additional separators allow greater flexibility in controlling the beam angles as they enter the IPs.

HIGHER SEPARATOR GRADIENTS

Running the separators at higher gradients is the most direct way to increase beam-beam separation. Higher separator voltages can increase the amplitude of the orbit helix, and, hence, the separation between the protons and antiprotons. The separator voltages must be scaled to maintain the 3-bump (or 4-bump) closure conditions in the arcs. It turns out that the separation scales as the voltage of the IP separators, i.e., scaling the helix such that the IP separator voltages increase by 10% results in a 10% increase of the separation.

Although the power supplies are limited to provide a 60 kV/cm maximum gradient, the breakdown (spark) rate of the separators determines the practical maximum of the gradient. When a spark occurs between the two plates of a separator during an HEP store, the resulting orbit deviation can drive beam into collimators (typically placed < 1 mm from the beam tails), causing a quench of nearby superconducting magnets and loss of the store. The breakdown rate rises exponentially with gradient; we would likely tolerate at most 1 spark per month among all the separators during HEP stores. This practical maximum should be determined operationally by trying higher separator voltages and retreating if the spark rate becomes intolerable.

We have recently run a number of HEP stores with collision helix sizes (90%, 100%, and 110% of nominal) in order to investigate the impact on operations. As expected, the tune changes caused by feeddown effects

for the different orbits were small (<0.0003), so we did not need to compensate the working point of the machine. Studying many stores allowed us to sample over a range of conditions, e.g., luminosities, beam intensities and emittances. For example, Figure 2 shows the initial luminosity lifetime, obtained from an exponential decay fit from the CDF experiment's luminosity counters, as a function of the initial luminosity and the so-called effective emittance of the beams. The effective emittance is defined as:

$$\varepsilon_{eff} = \frac{10^{-5} * f * B * N_P * N_A * (6\beta\gamma)}{4\pi\beta^* L} H\left(\sigma_z/\beta^*\right), \quad (2)$$

where f is the revolution frequency, $B = 36$ is the number of bunches, N_P is the number of protons per bunch, N_A is the number of antiproton per bunch, $\beta^* = 35$ cm is the design beta function at the IPs, L is the luminosity, $(6\beta\gamma)$ is the kinematic factor for calculating 95% emittance, and H is the hourglass factor depending upon the bunch lengths σ_z and β^*. Effective emittance is a measure of the particle intensities per unit luminosity; the lower the effective emittance, the more luminosity per beam particle. The correlations are obvious: luminosity lifetime decreases for larger luminosities and smaller effective emittances. The range of effective emittances stems primarily from the number of antiproton bunches originating from the Accumulator and the Recycler; antiprotons from the Recycler typically have transverse emittances 5-8 π mm mrad smaller than those from the Accumulator. The brighter Recycler antiprotons lead to Tevatron stores with smaller effective emittance stores.

In order to see any effect of the helix size on the luminosity lifetime, we looked at lifetime in different
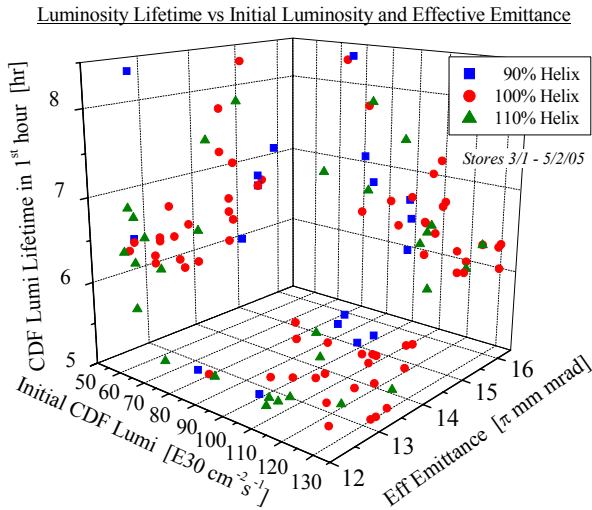
Figure 2: Luminosity lifetime in the first hour for the CDF experiment as a function of the initial luminosity and effective emittance for many HEP stores with different collision helix sizes; only the projections onto the three planes are shown. The luminosity lifetime was obtained from a fit to an exponential decay. The statistical uncertainties of the luminosity lifetime values are all less than 0.1 hr.
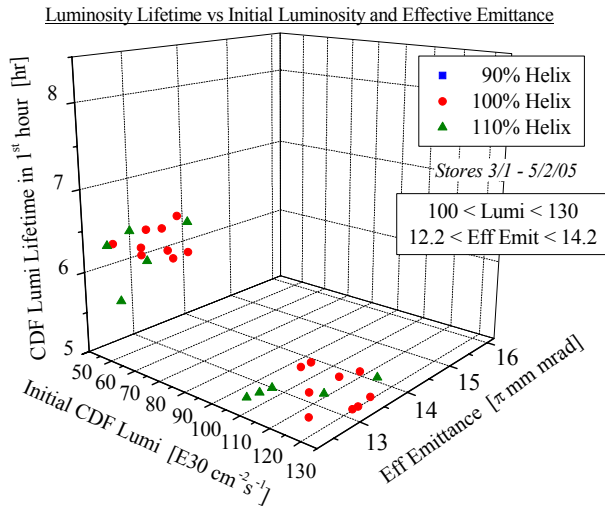

Figure 3: Luminosity lifetime in the first hour for the CDF experiment for a specific set of initial luminosities and effective emittances; only projections onto two planes are shown. No 90% helix stores are in this population of stores.

ranges of initial luminosity and effective emittance. The benefit of 110% versus 100% helix is not obvious, but it seems clear that the 90% helix results in lower luminosity lifetimes. Figure 3 shows the initial luminosity lifetimes for the stores with the highest initial luminosities and the smallest effective emittances. The approximate 1 hour spread in lifetimes for a given helix size makes it difficult

to identify the smaller (few tenths of an hour) expected improvements from the 110% helix.

The benefits of a larger helix size are more obvious when looking at the so-called non-luminous loss rate of the antiprotons. The non-luminous loss rate represents how quickly particles are lost from sources other than being "burned-up" in proton-antiproton collisions at the IPs. Figure 4 demonstrates how the non-luminous antiproton losses decrease as the helix size increases. The antiproton non-luminous loss rate early in a store is dominated by burn-up in collisions (≈4 %/hr), and it also depends on the antiproton emittances [4]. The non-luminous lifetime of proton bunches does not depend on the helix size.
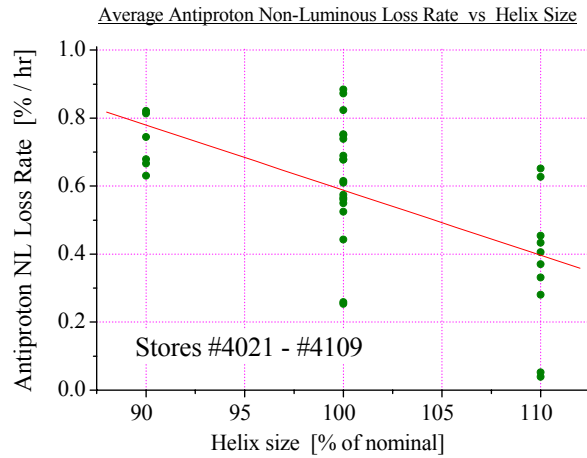

Figure 4: Average non-luminous loss rate of the 36 antiproton bunches in the first hour of many HEP stores for various collision helix sizes. The red line is the result of a linear fit.

CONCLUSION

In order to decrease long-range beam-beam effects in the Tevatron during HEP stores, we are attempting to increase the separation between the protons and antiprotons at the parasitic crossing points. Additional electrostatic separators are being installed into the arcs during long maintenance shutdown periods to gain up to 15% more separation. In addition, running the separators at higher voltages also increases the separations around the ring. We do observe improved non-luminous lifetimes for antiprotons with 10% higher separator voltages. The ultimate separation increase via higher voltages depends upon separator spark rates which increases exponentially with voltage across the gap.

REFERENCES

[1] D. McGinnis, these Proceedings (MOAA005).
[2] Y. Alexahin, these Proceedings (MOPA006).
[3] A. Valishev *et al.*, these Proceedings (TPAT083).
[4] V. Shiltsev *et al.*, these Proceedings (TPAP032).

Some ESS Conclusions

Muon Collider ESS much simpler problem than Tevatron

    fewer bunches

    no need for double helix

    pretzel will work fine (only 1 plane as in CESR, LEP,…)

    fewer turns so needed separation less (ms not hours)

    no ramping of collider, constant ESS Fields

    one spark does not destroy a day's work

shielding from upstream radiation may be needed, but

    if the pretzel is vertical, ESS midplane can be free

decay electrons within the ESS can be kept from plates

     with a small superimposed dipole field (new SBIR?)

Some ESS Conclusions (cont.)

Collider simulations needed to get Δv requirements

Lattice should have space for pretzel ESSs

ESS shielding requirements need to be estimated

Beam-induced ESS breakdown needs to be estimated/measured